

Spring 1-1-2013

# The Effects of Stream Channel Conductance on Stream Depletion

Gregory Dean Lackey

*University of Colorado at Boulder*, [gregory.lackey@colorado.edu](mailto:gregory.lackey@colorado.edu)

Follow this and additional works at: [https://scholar.colorado.edu/cven\\_gradetds](https://scholar.colorado.edu/cven_gradetds)

 Part of the [Environmental Engineering Commons](#), [Geomorphology Commons](#), and the [Hydraulic Engineering Commons](#)

---

## Recommended Citation

Lackey, Gregory Dean, "The Effects of Stream Channel Conductance on Stream Depletion" (2013). *Civil Engineering Graduate Theses & Dissertations*. 305.

[https://scholar.colorado.edu/cven\\_gradetds/305](https://scholar.colorado.edu/cven_gradetds/305)

This Thesis is brought to you for free and open access by Civil, Environmental, and Architectural Engineering at CU Scholar. It has been accepted for inclusion in Civil Engineering Graduate Theses & Dissertations by an authorized administrator of CU Scholar. For more information, please contact [cuscholaradmin@colorado.edu](mailto:cuscholaradmin@colorado.edu).

**The Effects of Stream Channel Conductance on Stream  
Depletion**

by

**Gregory Dean Lackey**

B.S., Environmental Systems Engineering

A thesis submitted to the  
Faculty of the Graduate School of the  
University of Colorado in partial fulfillment  
of the requirements for the degree of

Master of Science

Department of Civil Environmental and Architectural Engineering

2013

This thesis entitled:  
The Effects of Stream Channel Conductance on Stream Depletion  
written by Gregory Dean Lackey  
has been approved for the Department of Civil Environmental and Architectural Engineering

---

Roseanna M. Neupauer

---

John Pitlick

---

Harihar Rajaram

Date \_\_\_\_\_

The final copy of this thesis has been examined by the signatories, and we find that both the content and the form meet acceptable presentation standards of scholarly work in the above mentioned discipline.

Lackey, Gregory Dean (M.S., Environmental Engineering)

The Effects of Stream Channel Conductance on Stream Depletion

Thesis directed by Prof. Roseanna M. Neupauer

In regions where growing population and changing climate threaten freshwater supplies, accurate modeling of potential human impacts on water resources is necessary to ensure a sufficient supply of clean water. Stream depletion, the reduction of stream flow due to the extraction of groundwater from a hydraulically connected aquifer, can reduce water availability; thus, accurate modeling of stream depletion is an important step in siting new groundwater wells. Proper estimation of stream depletion requires appropriate parameterization of aquifer and streambed hydraulic properties. Although streambed hydraulic conductivity ( $K_r$ ) varies spatially and temporally in natural streams, many numerical investigations of stream depletion assume or calibrate for a single representative value of  $K_r$ . In this work, we use MODFLOW-2000 to demonstrate that ranges of  $K_r$  exist to which stream depletion estimations are sensitive and insensitive. We show that the sensitivity of a model to  $K_r$  is dependent upon the model input parameters. Considering the uncertainty that is introduced from the assumption or calibration of a parameter, we apply concepts from sediment transport theory to develop modeling methods that more accurately represent the spatial and temporal heterogeneity of the stream channel. We compare stream depletion estimations from various heterogeneous  $K_r$  scenarios with a homogeneous base case to investigate how the different modeling schemes impact the feasibility of pumping well locations in the aquifer. Modeling patterns of  $K_r$  heterogeneity significantly alters stream depletion estimations. However, accounting for temporal variations in heterogeneity patterns lessens the degree to which heterogeneity along the stream channel impacts stream depletion estimations.

## Dedication

To my parents who have supported me in all of my academic pursuits.

## Acknowledgements

Thanks first and foremost to my adviser, Roseanna Neupauer. Without her guidance and feedback this work would not be possible. Thanks also to the United States Geological Survey for funding this project under the Water Resources Research Institute Program, Project No. 2009CO195G. Finally, thanks to my family and friends who have enriched my life in an endless number of ways.

# Contents

## Chapter

<b>1</b>	Introduction	1
1.1	Motivation . . . . .	1
1.2	Background . . . . .	3
1.2.1	Hydraulically Connected Surface and Groundwater Flow . . . . .	3
1.2.2	Stream Depletion . . . . .	3
1.2.3	Analytical Approaches for Estimating Stream Depletion . . . . .	4
1.2.4	Numerical Approaches for Estimating Stream Depletion . . . . .	7
1.2.5	Relationship Between Stream Channel Conductance and Stream Depletion . . . . .	8
1.2.6	Stream Channel Heterogeneity . . . . .	11
1.2.7	Modeling Stream Channel Heterogeneity . . . . .	13
1.3	Problem Statement . . . . .	15
1.4	Project Goals . . . . .	15
1.5	Scope . . . . .	16
1.6	Organization of this Thesis . . . . .	16
<b>2</b>	Sensitivity of Stream Depletion Estimations to Streambed Hydraulic Conductivity	17
2.1	Introduction . . . . .	17
2.2	Conceptual Model . . . . .	18
2.3	Equations for Calculating Stream Depletion . . . . .	20

2.4	Results . . . . .	23
2.5	Discussion . . . . .	27
2.6	Summary . . . . .	31
<b>3</b>	<b>Effects of Stream Channel Heterogeneity on Stream Depletion:</b>	
	Heterogeneity Along the Stream Channel	32
3.1	Introduction . . . . .	32
3.2	Conceptual Model . . . . .	33
3.3	Effects of River Flow Regime on Stream Depletion . . . . .	33
3.4	Effects of a Temporally Variable River Flow Regime on Stream Depletion . . . . .	39
3.5	Practical Implications . . . . .	45
3.6	Summary . . . . .	46
<b>4</b>	<b>Discussion, Conclusions and Future Work</b>	<b>50</b>
4.1	Assumptions . . . . .	50
4.2	Limitations . . . . .	50
4.3	Conclusions . . . . .	52
4.4	Future Work . . . . .	53
	<b>Bibliography</b>	<b>54</b>



## Tables

### Table

2.1	Summary of non-variable model parameters . . . . .	20
2.2	Summary of variable model parameters . . . . .	21
3.1	Temporal setup of models . . . . .	40

## Figures

### Figure

1.1	Cross sectional view of the streambed. . . . .	9
2.1	Plan view of modeled aquifer . . . . .	19
2.2	Initial distribution of hydraulic head in aquifer . . . . .	24
2.3	Stream depletion as a fraction of the pumping rate vs. time . . . . .	24
2.4	Hypothetical model aquifer . . . . .	27
2.5	Stream depletion vs. $\log \Gamma$ for 29 scenarios with different $\Lambda$ values . . . . .	29
3.1	Plan view of the assumed $K_r$ heterogeneity patterns along the streambed . . . . .	34
3.2	Stream depletion estimated at every well location in model domain for variations of $K_r$ within the sensitive range and along the stream channel . . . . .	36
3.3	Stream depletion estimated at every well location in model domain for variations of $K_r$ along the stream channel above the sensitive range . . . . .	37
3.4	Stream depletion vs. time in an aquifer with temporally variable $K_r$ . . . . .	41
3.5	Stream depletion estimated at every well location in model domain for temporal simulations in which the high flow regime is varied on a half-year basis . . . . .	42
3.6	Stream depletion estimated at every well location in model domain for temporal simulations in which the high flow regime is varied on a quarter-year basis . . . . .	43
3.7	Comparison of feasible pumping well locations between homogeneous and heterogeneous $K_r$ scenarios . . . . .	47

3.8 Comparison of feasible pumping well locations between homogeneous and temporally variable heterogeneous $K_r$ scenarios . . . . .	48
--	----

## Chapter 1

### Introduction

#### 1.1 Motivation

At an approximate volume of  $2.78 \times 10^{18}$  gallons, groundwater comprises 30.1% of global fresh water and is the worlds largest unfrozen store of fresh water (NGWA, 2010). The generally high quality and widespread availability of groundwater make it an invaluable asset. Currently, groundwater makes up one third of all freshwater consumption and is used to meet 42% of the agricultural demand, 36% if the global domestic demand, and 27% of the industrial water demand (Taylor et al., 2012). The United States (US) relies heavily on groundwater, using 79.6 billion gallons each day (NGWA, 2010). In the US, groundwater is used for 33% of public and 99% of domestic drinking water as well as for 60% of irrigated land (Kenny et al., 2009; Scanlon et al., 2012).

The value of groundwater lies in its high quality and ability to be extracted without negatively impacting the surrounding environment. In river valleys, a hydraulic connection often exists between groundwater and surface waters. This connection can become a concern in regions where groundwater is withdrawn to the extent that surface water flow is depleted. This phenomenon is known as stream depletion and it can have a number of negative environmental and legal implications (Barlow and Leake, 2012).

Groundwater baseflow is essential for creating the stream conditions required to sustain fish and other aquatic organisms. Throughout the year, groundwater has a relatively stable temperature and it serves to regulate the temperature fluctuations of surface water. Groundwater also stabilizes

the chemistry of streams by contributing alkalinity which buffers the system from acidic inputs. A significant reduction in groundwater flow can alter the resilience of a stream to these external factors and destroy the affected ecosystem (Barlow and Leake, 2012).

In the US, the legality of impacting surface water flow via groundwater extraction is dependent upon the established water rights within each state. For example, the water rights defined by the State of Colorado distinguish between tributary and non-tributary groundwater. A tributary groundwater source depletes the stream flow of a hydraulically connected stream by 0.1% of the annual rate of withdrawal in a single year over a one hundred year period. If a source is determined to be tributary groundwater, it is regulated under the same legislative rights as surface water. Conversely, non-tributary groundwater is not subject to surface water rights and can be used in different ways (Colorado Revised Statute Section 37-90-103-10.5).

Water rights are particularly important for states in the arid west or southwest that have access to fewer water resources (Brookshire et al., 2002). Over the past decade temperatures in the southwest increased and precipitation events have become less frequent and more volatile. Climate models predict that droughts in the 21st century will last longer and be more intense. These states will continue to see an increased demand for groundwater as more of it will be needed to buffer against the increasing scarcity of freshwater (MacDonald, 2010).

Populations are predicted to grow in the western US as well, leading to a further increased demand of freshwater. The most recent census confirmed that western cities are growing faster than eastern cities as a result of migration. It is projected that between 2000 and 2030 the western and southern US will grow by approximately 46% and 43%, respectively. Growth in these regions will account for 29% of the forecasted population rise in the US over this time period (Hansen 2012). Installing new wells in these regions to meet the freshwater demand increases the risk of depleting surface waters.

## **1.2 Background**

### **1.2.1 Hydraulically Connected Surface and Groundwater Flow**

Surface and subsurface water are inherently connected in the hydrologic domain. These two entities typically interact in the hyporheic zone where flow occurs laterally between groundwater and surface water. Exchange of water through the hyporheic zone is driven by the relationship between the hydraulic head of the surrounding aquifer and the stage of the river. Flow is controlled by the hydraulic properties of the the stream channel and the surrounding rock (Cardenas, 2009).

Subsurface flow must travel through the pore space in rocks and is generally slow-moving. The patterns of groundwater flow are controlled by the shape of the water table, which develops as a diminished imitation of the land surface, and the hydraulic conductivity of the surrounding sediment. If the hydraulic head in an aquifer underlying a stream is higher than the stream level, groundwater flows into the stream channel and contributes to surface water flow. This groundwater is classified as baseflow and it often maintains stream flow between precipitation events.

Surface water flow properties are directly influenced by precipitation, snow melt and baseflow. Water flowing through a surface channel typically moves significantly faster than groundwater as it is generally unobstructed. Streams that are partially comprised of groundwater are considered to be gaining streams. Gaining streams persist as long as the hydraulic head in the aquifer is larger than the hydraulic head in the stream. However, if this relationship is reversed, a stream can be converted to a losing stream. The hydraulic head of a losing stream is higher than the hydraulic head in the surrounding aquifer and water from the losing stream flows into the surrounding aquifer (Sophocleous, 2002).

### **1.2.2 Stream Depletion**

Extracting groundwater from an aquifer results in a depression of hydraulic head that forms in the shape of a cone around the pumping well. If a stream is hydraulically connected to the impacted aquifer, this depression can disturb the hydraulic relationship between the surface and

groundwater. Often, baseflow that contributes to flow in a gaining stream is intercepted, which consequently lowers the flow rate of the stream. If the hydraulic head depression in the aquifer is large enough, the hydraulic gradient near the stream channel can be reversed. This causes water flowing in the stream to infiltrate into the adjacent aquifer, transforming the gaining stream into a losing stream. The quantity of water captured by the pumping well that no longer contributes to surface water flow is referred to as stream depletion.

### 1.2.3 Analytical Approaches for Estimating Stream Depletion

Theis (1941) was the first study to develop an analytical method for quantifying stream depletion. The Theis (1941) expression was created for stream depletion in a unconfined aquifer of infinite extent that was assumed to be homogeneous and isotropic with a uniform thickness. Neither recharge nor evapotranspiration were considered. The impacted hypothetical stream was assumed to fully penetrate the aquifer in a straight line that extended beyond the influence of the pumping well. It was also assumed that the hydraulic head of the stream remained constant and that the streambed sediments provided no resistance to flow between the aquifer and the stream. The pumping well was approximated as a point that fully penetrated the aquifer. Theis (1941) concluded that the degree to which depletion occurs in a stream is a factor of the transmissivity of the aquifer and the distance between the pumping well and the stream.

Glover and Balmer (1954) maintained the same assumptions as Theis (1941) and developed another analytical expression of stream depletion. In their version of the equation, Glover and Balmer express stream depletion as a fraction of the total rate of extraction from the well which makes the parameter dimensionless. Jacob (1950) approximated the head loss caused by the resistance of flow across the streambed by assuming an increased distance between the pumping well and the stream. This assumption was flawed because the additional section of aquifer between the pumping well and stream provided more storage, which altered depletion estimations. Hantush (1965) adjusted for these inaccuracies by assuming a layer that created the needed resistance between the stream channel and aquifer but had insignificant storage capacity. The author

also suggested ways that the analytical solution could account for a partially penetrating stream channel.

Multiple field studies have illustrated the flaws in the assumptions of the Theis (1941) and Glover and Balmer (1954) expressions. Moore and Jenkins (1966) investigated the applicability of assuming a fully penetrating streambed with perfect hydraulic connection. Using a section of the Arkansas River, the authors demonstrated how easily the water table can drop below a streambed and cause an imperfect hydraulic connection. Sophocleous et al. (1988) showed that in a true stream-aquifer system, a pumping well can draw water from the opposite side of the stream. Their results indicated that the available analytical solutions were overestimating stream depletion because they could not account for the extra storage beyond the impacted stream.

Spalding and Khaleel (1991) was the first numerical study to tie together the criticisms of the analytical solutions. The authors compared stream depletion estimations made using the analytical equations from Theis (1941), Glover and Balmer (1954), Jacob (1950) and Hantush (1965) with estimations from a two-dimensional groundwater flow model. Spalding and Khaleel (1991) found that each of the analytical approaches overestimated stream depletion. Theis (1941) and Glover and Balmer (1954) were the most inaccurate approaches because the two methods neglected the hydraulic resistance of the streambed sediment. Other inaccuracies arose with all four analytical methods because of their inability to account for partially penetrating streambeds and their neglect of storage in regions beyond the stream. The Spalding and Khaleel (1991) study served two purposes; (1) It showed the inaccuracies of the analytical approaches for estimating stream depletion; (2) it illustrated how useful numerical models could be for stream depletion calculations.

Hunt (1999) and Zlotnik and Huang (1999) were the first studies to develop analytical solutions for stream depletion that accounted for partially penetrating stream channels with sediment layers that provided flow resistance between the aquifer and the stream. The primary difference between the two methods was the assumption of an infinitesimal stream, made by Hunt (1999). Hunt (2003) developed a solution for application to a scenario in which groundwater is extracted from



a confined aquifer. In his study, the streambed partially penetrates the semi-permeable confining layer (Hunt, 2003).

Butler et al. (2001) considered a confined isotropic aquifer of finite extent interfacing with a stream of a predetermined width. A small degree of river penetration was assumed in the work and the head of the river remained constant. It was found that an aquifer would need to be two or three orders of magnitude larger than the stream width before the assumption of an aquifer of infinite extent would apply. The study also investigated the error introduced by the Theis (1941) assumption of a fully penetrating streambed and found that this method can over estimate stream depletion by 100-1000% when applied to a true system.

Zlotnik (2004) investigated the maximum stream depletion rate (MSDR) parameter, which is the maximum degree to which stream depletion contributes to groundwater withdrawal in a stream-aquifer system. The author demonstrated that leakage from nearby aquifers can supply recharge to an aquifer leading to MSDR values that range from 0 to 100%. The study concluded that the MSDR is dependent upon the proximity of the well to recharge sources and the hydraulic conductivity of the aquitard.

Butler et al. (2007) incorporated the effects of an underlying leaky aquitard, highlighted by Zlotnik (2004), by developing a semi-analytic method which showed that the amount of water that is contributed to a pumping well from underlying aquifer leakage increases with the distance between the pumping well and the stream. Therefore, in stream-aquifer systems with underlying confined aquifers, a pumping well can be placed a distance from the stream where aquitard recharge contributes more water to the pumping well than stream depletion. This distance is a factor of the hydraulic properties of the aquifer and aquitard. Considering the potentially large size of the aquitard, it was found that uncertainties in its conductivity could greatly affect stream depletion calculations. Zlotnik and Tartakovsky (2008) furthered this method by developing steady-state and transient solutions for stream depletion and drawdown that allowed for the individual quantification of the effects of streambed conductance, aquitard conductivity, and streambed penetration.

Butler et al. (2001, 2007) assumed that no drawdown occurs in the underlying confined

aquifer. Hunt (2009) showed that this assumption does not mimic the delayed yield of a true system, and developed a semi-analytical expression that accounts for drawdown in the confined aquifer. Ward and Lough (2011) used the Hunt (2009) solution to show the effects of assuming horizontal flow in the unconfined aquifer on long term stream depletion estimations. The authors concluded that this assumption may reduce the long term predictions of drawdown in the confined and unconfined aquifers resulting in larger estimations of stream depletion.

A few semi-analytical approaches have been developed to understand how various stream configurations affect stream depletion. Sun and Zahn (2007) investigated a scenario in which pumping occurs between two parallel rivers. The study found that the ratio between the streambed hydraulic conductivity, and to a lesser degree the streambed thicknesses, dictate which stream is the dominant water supplier to the well. Yeh et al. (2008) also developed a semi-analytical approach for estimating stream depletion in a multi-stream aquifer where the streams come together to form a wedge shape. They concluded that the angles of the streams play a role in the total stream depletion rate that can occur at the pumping well.

#### **1.2.4 Numerical Approaches for Estimating Stream Depletion**

Spalding and Khaleel (1991) was the first study to demonstrate the usefulness of numerical models for estimating stream depletion. The authors compared stream depletion calculations from AQUIFEM, a two-dimensional groundwater flow model, with results from three commonly used analytical approaches. It was found that the numerical approach was more accurate than the analytical methods for estimating stream depletion because of its ability to operate under fewer assumptions. Sophocleous et al. (1995) and Conrad and Beljin (1996) performed similar analyses comparing analytical stream depletion estimations with results from the numerical model MODFLOW. Sophocleous et al. (1995) investigated the accuracy of Glover and Balmer's analytical method and Conrad and Beljin (1996) focused on how changes in areal recharge and streambed conductance impact analytical estimations. Each of these works exposed the shortcomings of analytical stream depletion solutions and demonstrated the usefulness of numerical models for estimating

stream depletion.

Considering the complex nature of stream-aquifer systems and the ability of numerical models to simulate them, MODFLOW has become the standard tool used for estimating stream depletion. A number of studies have used MODFLOW to better understand the effects of various hydraulic conditions on stream depletion calculations. Chen and Yin (1999) highlighted the significance of accurate aquifer vertical hydraulic conductivity values on stream depletion estimations. For example, Chen and Yin (2001) and Chen and Shu (2002) analyzed how aquifer hydraulic properties affect baseflow reduction and induced streambed infiltration.

Leake et al. (2008), Lambert et al. (2011) and Neilson and Locke (2012) use MODFLOW to estimate the degree of stream depletion that would be caused by pumping in the Upper San Pedro Basin, the Uinta River Valley, and the watershed surrounding Freeport, Maine, respectively. Studies that model region-scale estimations of stream depletion typically calculate the degree of stream depletion caused by pumping at every location in the model domain. This requires separate forward runs of the model for each potential well location. The calculations required to perform these simulations become more cumbersome, take more time, and use up more computer memory as the size and complexity of models increase. Neupauer and Griebeling (2012) and Griebeling and Neupauer (2013) developed the adjoint approach for estimating stream depletion. The approach calculates stream depletion throughout an entire region in a single adjoint simulation, which saves time as well as computer memory.

### 1.2.5 Relationship Between Stream Channel Conductance and Stream Depletion

The degree to which a stream or river is depleted by a nearby pumping well depends on the hydraulic properties of the streambed. All water entering or leaving the stream channel must pass through the sediments in the streambed which typically have different characteristics than the surrounding aquifer. Flow from the stream into the aquifer ( $Q_s$ ) is quantified using Darcy's law

$$Q_s = \frac{wLK_r}{b_r}(h_s - h) \quad (1.1)$$

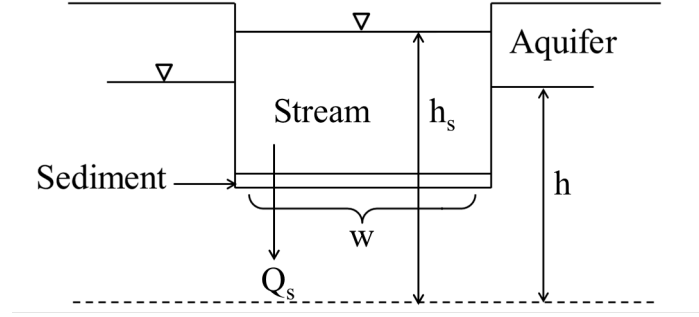


Figure 1.1: Cross sectional view of the streambed.

where  $w$  is the width of the stream channel,  $K_r$  is the streambed hydraulic conductivity,  $b_r$  is the thickness of the streambed sediment,  $L$  is the length of stream reach,  $h_r$  is hydraulic head in the stream and  $h$  is hydraulic head in the aquifer. Figure 1.1 shows a schematic of a stream channel that is losing water to the surrounding aquifer due to  $h$  being lower than  $h_r$ .

Groundwater pumping often results in the lowering of  $h$ , which alters  $Q_s$ . Although the river has multiple sources and sinks of water, such as lateral inflows, precipitation, and evaporation, only  $Q_s$  is affected by groundwater extraction. Therefore, the degree to which a stream is depleted is equivalent to the change in  $Q_s$  as a result of pumping.

Equation 1.1 shows that the value of  $Q_s$ , and therefore stream depletion, is dependent on the hydraulic properties of the streambed as well as the hydraulic head difference between the stream and the surrounding aquifer. The hydraulic heads of the aquifer and stream vary spatially and temporally and are typically calculated in groundwater flow models. Therefore,  $w$ ,  $K_r$ , and  $b_r$  are the input parameters of a modeled streambed that have the most impact on the degree to which stream depletion occurs in the stream.

These important hydraulic properties of the stream,  $K_r$ ,  $L$ ,  $b_r$  and  $w$ , are lumped together in a single term, the stream channel conductance,  $C$ , which is given by

$$C = \frac{wLK_r}{b_r}. \quad (1.2)$$

Many analytical and numerical studies cite  $C$  as one of the most important model parameters for accurately estimating stream depletion (e.g. Spalding and Khaleel, 1991; Sophocleous et al., 1995;

Hunt, 1999; Zlotnik and Huang, 1999; Butler et al., 2001). Christensen (2000) investigated the sensitivity of analytical stream depletion estimations to  $C$ . The study found that stream depletion calculations in aquifers with large and small storativity are extremely sensitive variations in  $C$ . Considering the implications that the parameter has on stream depletion estimations, it was determined that  $C$  provided the greatest source of uncertainty for stream depletion models (Christensen, 2000).

Chen and Yin (1999) investigated the effects of  $C$  on numerical stream depletion estimations through variations in  $K_r$ . Although it was not the focus of their work, they used MODFLOW to demonstrate that streams with low  $K_r$  experience less stream depletion (Chen and Yin, 1999). Chen and Shu (2002) studied how  $C$  impacts numerical stream depletion estimations. The study focused on understanding how  $C$  affects the pathways of stream depletion, stream infiltration and baseflow interception. The authors found that induced stream infiltration contributes a greater percentage of the total stream depletion at higher  $C$ . Conversely, at lower  $C$  baseflow reduction contributes more to stream depletion. The study also concluded that a higher  $C$  generally causes a better connection between the stream and aquifer, which results in an increase of stream depletion. However, the increase in stream depletion is not proportional to the increase in  $C$ . Stream depletion increases at a decreasing rate with increasing  $C$  and reaches a maximum that is determined by the hydraulics of the aquifer (Chen and Shu, 2002).

Chen et al. (2008) measured changes in the vertical component of  $K_r$ ,  $K_v$ , with depth in the streambed of southeast Nebraska's Platte River. The study found that the streambed is stratified with layers of variable  $K_v$  that typically decrease with depth. The authors investigated the effects of a variety of  $K_v$  units on stream depletion. It was found that stream depletion is reduced when the low  $K_v$  layer occurs closer to the channel surface. The value and extent of the low  $K_v$  layer also affects stream depletion. Less stream depletion was observed when the  $K_v$  of the layer decreases and the extent to which it covers the bottom of the stream channel was increased.

### 1.2.6 Stream Channel Heterogeneity

As rivers and streams move across their floodplains they drain water from the land and act as a primary source of transport for the products of weathering. Eroded sediments suspended in these moving bodies of water are what eventually comprise the streambed. Various geomorphologic features of the stream such as riffles, pools, bends and straight sections can influence the flux of sediments between the stream and its underlying channel. A constant cycle of sediment entrainment and deposition creates a heterogeneous stream channel that is in a continuous state of change (Andrews, 1979).

The hydraulic characteristics of the streambed are depicted by the properties of the residing sediments. Particle size affects the streambed hydraulic conductivity,  $K_r$ , and the natural filling and scouring of sediments determines the thickness of the streambed sediments,  $b_r$ . Both of these parameters directly impact the streambed conductance. As a result, the direction and magnitude of groundwater fluxes between a stream and its nearby aquifer vary spatially and temporally in the stream channel (Palmer, 1993).

Numerous field studies have confirmed the highly heterogeneous nature of the stream channel through measurements of both the horizontal ( $K_h$ ) and vertical ( $K_v$ ) components of sediment  $K_r$  (Springer et al., 1999; Cardenas and Zlotnik, 2003; Chen, 2004; Chen, 2005; Ryan and Boufadel, 2006; Genereux et al., 2008; Chen et al., 2008; Cheng et al., 2011). Flow across the stream channel is controlled by  $K_v$  and flow within the stream channel is controlled by  $K_h$ . Numerical stream depletion estimations rely on  $K_v$  and studies investigating surface-subsurface solute interaction are interested in  $K_h$ .

Concrete patterns in  $K_r$  could not be established widely across each study; however, some trends were observed. Genereux et al. (2008) recorded  $K_v$  measurements of West Bear Creek in North Carolina over the course of one year. The study recorded a spatial variation in  $K_v$  and concluded that the size and distribution of the sediments created a streambed where  $K_v$  was generally higher in the center of the stream channel. Ryan and Boufadel (2006) measured the  $K_h$

of two distinct streambed layers of Indian Creek in eastern Pennsylvania. The authors found that  $K_h$  decreased with depth and were significantly larger in the upper sediment layer. This trend of decreasing  $K_r$  with streambed depth was also observed in Chen et al. (2008) and Chenpeng et al. (2011), two studies that measured  $K_v$  of the Platte River in southeast Nebraska.

A variety of statistical relationships for  $K_h$  and  $K_v$  have been observed in the field data collected. Springer et al. (1999) found that  $K_h$  of reattachment bar sediments in the Grand Canyon segments of the Colorado River followed a bimodal distribution. The vertical streambed hydraulic conductivity distribution observed by Genereux et al. (2008) in West Bear Creek also suggested a bimodal trend. Cardenas and Zlotnik (2003) measured streambed  $K_h$  in the Prairie Creek of Nebraska. Their data followed a normal distribution, which agreed with the trend found in  $K_v$  data collected by Chen (2005) in the Nebraska reaches of the Platte River. Ryan and Boufadel (2006) determined that  $K_h$  was log-normally distributed in each of the separate sediment layers of Indian Creek but not for their combined dataset. Cheng et al. (2011) developed a statistical relationship for  $K_v$  values along a 300 km stretch of the Platte River in Nebraska. The authors recorded numerous measurements of  $K_v$  a set distance apart at each testing site and found that  $K_v$  values at every sampling site in the Platte River were normally distributed when outlying data was not considered. Combined datasets from each location were only found to be normally distributed above the tributary confluences. A non-normal distribution was found in combined datasets that included locations above and below tributary inputs.

The temporal variability of streambed hydraulic properties have also been investigated (Springer et al., 1999; Doppler et al., 2007; Genereux et al., 2008; Mutiti and Levy, 2010; Levy et al., 2011; Simpson and Meixner, 2012). Genereux et al. (2008) measured streambed  $K_v$  bimonthly over the course of one year and recorded significant temporal variations. The effects of individual flow events on streambed  $K_r$  were investigated by Springer et al. (1999), Doppler et al. (2007), Mutiti and Levy (2010), and Simpson and Meixner (2012). These studies concluded that streambed  $K_v$  gets larger during increased flow events such as storms and floods. Treese et al. (2009) suggests that the increase in  $K_v$  during high flow events is a result of the removal of the clogging layer that is formed

by physical, chemical and biological processes. Simpson and Meixner (2012) modeled a synthetic flood event and monitored the effects of hydraulic conditions and particle size on the deposition of sediments. The study found that during the rising limb of a flooding event, fine particles are entrained while coarse sediments remain on the channel bottom. This results in an increase of  $K_v$ . Conversely, during the falling limb of a flooding event, fine sediments are reestablished on the stream bottom resulting in a lowering of the stream channel  $K_v$ .

Despite the inability of hydrogeology field studies to identify spatial and statistical relationships for measured streambed  $K_r$ , trends in sediment transport have been observed by stream geomorphologists. The pool and riffle sequence, described by Andrews (1979), has been used to characterize sediment transport under various flow conditions. Pools are defined as sections of the stream that are deeper and wider. Under low flow conditions finer sediments are typically deposited on the stream channel beneath pools. Riffles are thinner shallower sections of the stream. Sediments are scoured from riffles during low flow conditions leaving behind coarse bed material. High flow conditions reverse these transport trends in pools and riffles. Sediments are entrained in pools and deposited in riffles (Andrews, 1979; Sear, 1996; Clayton and Pitlick, 2007).

### 1.2.7 Modeling Stream Channel Heterogeneity

Over the past twenty years river ecologists and hydrogeologists have strived to characterize the streambed. Ecologists have focused their work on understanding the interactions that occur in the hyporheic zone at the interface between groundwater and surface waters (Palmer, 1993; Harvey and Bencala, 1993). While hydrogeologist and water resource managers have worked on improving stream depletion estimations through the modeling of a low permeability streambed (Sophocleous et al., 1995; Zlotnik and Huang, 1999; Hunt, 1999; Butler et al., 2001). However, many intricacies of streambed heterogeneity are still relatively unexplored. Sophocleous et al. (2002) reviewed the state of groundwater surface water interactions and emphasized delineation of the heterogeneous streambed as one of the most important areas in need of further research.

Some effort has been made to account for stream channel heterogeneity in numerical models.



Cardenas and Zlotnik (2003) used small scale hydraulic testing and structure-imitating interpolation to develop a representative three-dimensional MODFLOW model of saturated flow through streambed sediments. The study focused on a single stream channel bend and the results could not be applied to a larger investigation of stream depletion or hyporheic zone interactions. However, the authors did show that it is possible to develop better characterizations of the streambed.

Cardenas et al. (2004) used the three-dimensional heterogeneous streambed MODFLOW model to investigate channel-scale hyporheic zone processes. The authors focused on how heterogeneity, bed forms and stream curvature affect subchannel hyporheic exchange. This study showed how a MODFLOW model could be scaled down to simulate advection through the hyporheic zone, however, it was limited in that it could not be applied to a region scale simulation.

MODFLOW is the most commonly used numerical model for the simulation of surface water groundwater interactions (Brunner et al., 2010). While MODFLOW has been proven to be useful for small scale investigations of stream channel heterogeneity (e.g. Cardenas and Zlotnik, 2003; Cardenas et al., 2004), no studies have developed a region-scale method for modeling the heterogeneity that arises in a true streambed. Brunner et al. (2010) compared groundwater surface water exchange simulated in MODFLOW and in HydroGeoSphere (HGS), a groundwater flow model that is capable of simulating saturated and unsaturated flows. They found that MODFLOW is less accurate because of several underlying assumptions, including neglecting negative pressure gradients under the streambed, assignment of the modeled river to one grid cell, and vertical discretization of the model domain as factors that affect infiltration flux.

Irvine et al. (2012) used HGS to analyze the interaction between a heterogeneous section of stream and the surrounding alluvial aquifer. The authors compared the fluxes of surface water and groundwater that occur in heterogeneous and homogeneous streambeds surrounded by transitional water tables. The largest flow error observed as a result of the homogeneous assumption was 34%, which further emphasizes the importance of accounting for streambed heterogeneity.

### 1.3 Problem Statement

Extracting groundwater from an aquifer has the potential to reduce the flow rate of a hydraulically connected stream or river. This phenomenon is known as stream depletion and it occurs as a result of artificially lowered hydraulic head in the surrounding aquifer. Numerical models are used to perform stream depletion estimations because of their ability to simulate complex and realistic stream aquifer systems. Numerous studies have emphasized the importance of accurately representing the streambed in these models (e.g. Spalding and Khaleel, 1991; Sophocleous et al., 1995; Hunt, 1999; Zlotnik and Huang, 1999; Butler et al., 2001). However, in order to practically run simulations, modelers must make simplifying assumptions. It is often the case that the spatial variability of streambed hydraulic properties is not considered and homogeneous values are assumed or calibrated for instead (e.g. Fleckenstein et al., 2006; Leake et. al., 2008). This is not an accurate representation of a real streambed where sediment heterogeneity often leads to variations in  $K_r$  over several orders of magnitude (Fleckenstein et al., 2006). Calver (2001) demonstrated the variability of  $K_r$  by compiling the values of this parameter used in numerous field and numerical studies. The author found that  $K_r$  varied over seven orders of magnitude from  $1.0 \times 10^{-9} \text{ m s}^{-1}$  to  $1.0 \times 10^{-2} \text{ m s}^{-1}$  between the studies. As demonstrated by Equation 1.1, stream depletion estimations are potentially sensitive to the chosen value of  $K_r$ . Considering the significance of  $K_r$  in stream depletion estimations, questions arise about the validity of assuming a homogeneous stream channel.

### 1.4 Project Goals

The goal of this project is to:

1. Determine the sensitivity of numerical stream depletion estimations to variations in  $K_r$ .
2. Investigate the significance of accounting for spatial and temporal  $K_r$  heterogeneity in stream depletion models.

We use the widely adopted program MODFLOW-2000 to perform our simulations with the

aim of improving standard stream depletion estimation methods. It is our hope that the findings of this work will provide guidance for developing groundwater flow models that more accurately estimate stream depletion.

## 1.5 Scope

In this work we estimate stream depletion in a one layer, homogeneous, isotropic and unconfined aquifer. We assume a simplified aquifer to clearly identify how varying  $K_r$  impacts stream depletion. We run all of our stream depletion simulations using MODFLOW-2000 (Harbaugh et al., 2000). While programs like HydroGeoSphere (HGS) may be able to more accurately model the complexities that arise in a true stream aquifer system, MODFLOW is the standard program used by water resource managers to perform stream depletion simulations. We focus our work on MODFLOW simulations because we seek to understand the impact that assuming or calibrating for a homogeneous  $K_r$  value has on current stream depletion estimations.

## 1.6 Organization of this Thesis

The organization of this thesis is as follows. Chapter 2 investigates the effect of streambed hydraulic conductivity,  $K_r$ , on stream depletion estimations, for homogeneous stream channels. We use the range of  $K_r$  identified by Calver, and we demonstrate that the sensitivity of numerical stream depletion models to  $K_r$  is dependent upon model input parameters. Chapter 3 investigates the effect of modeling  $K_r$  heterogeneity on stream depletion. We vary  $K_r$  spatially and temporally, and we show the significance of accounting for heterogeneity when  $K_r$  varies over the sensitive range. Chapter 4 discusses assumptions and limitations of our work and Chapter 5 summarizes conclusions and discusses future work.

## Chapter 2

# Sensitivity of Stream Depletion Estimations to Streambed Hydraulic Conductivity

### 2.1 Introduction

We begin our investigation of the effects of streambed heterogeneity on stream depletion estimations by determining the sensitivity of these calculations to streambed hydraulic conductivity ( $K_r$ ). Flow across the stream channel is controlled by the streambed conductance ( $C$ ). Equation 1.2 shows that if all other parameters are held constant, variations in  $K_r$  directly correlate to variations in  $C$ . Numerous studies have emphasized the importance of accurately representing  $K_r$  in stream depletion estimations (e.g. Spalding and Khaleel, 1991; Sophocleous et al., 1995; Hunt, 1999; Zlotnik and Huang, 1999; Butler et al., 2001). The value of  $K_r$  is dictated by the hydraulic properties of the streambed sediments, and due to their highly heterogeneous nature, Christensen (2000) concluded that  $K_r$  is the most uncertain parameter in numerical stream depletion estimations. These studies suggest that the properties of the streambed play an important role in stream depletion calculations. However, Leake et al. (2008) demonstrated a scenario in which the degree of stream depletion estimated by a groundwater flow model was insensitive to the assumed  $K_r$ .

In this chapter we investigate the sensitivity of groundwater flow models to variations in  $K_r$ . Our goal is to assess the ranges of  $K_r$  to which our model is sensitive and insensitive and understand how these ranges are impacted by the model parameters. In Section 2.2, we describe a simplified one layer basin model with a meandering stream running through the center. We use this model in Section 2.3 to estimate how variations in  $K_r$  affect stream depletion estimations. We

assume a homogeneous streambed and run 29 simulations, for each of which we assign a different homogeneous  $K_r$  value. We analyze how pumping from a single well location in the aquifer causes stream depletion as a fraction of the pumping rate ( $\Delta Q_r/Q_p$ ) to occur with time and assess the values of  $K_r$  to which stream depletion calculations are sensitive and insensitive. We then alter the model input parameters and assess changes to the sensitive  $K_r$  range.

## 2.2 Conceptual Model

We develop a simple model, shown in Figure 2.1, to analyze the sensitivity of stream depletion calculations to variations in  $K_r$ . It is comprised of a single 500 m thick layer representing an isotropic, homogeneous, unconfined aquifer. We assume an aquifer hydraulic conductivity,  $K$ , and specific yield,  $S_y$ , of 50 m d<sup>-1</sup> and 0.2, respectively. The model domain spans from  $x = 0$  km to  $x = L_x = 160$  km in the  $x$  direction and  $y = 0$  km to  $y = L_y = 200$  km in the  $y$  direction. The model flow boundaries are set to imitate flow through a river basin. The north, east and west boundaries of the model are designated as no flow boundaries and the southern boundary is defined as a constant head boundary with  $h = 50$  m. Water enters the model through evenly distributed recharge of  $6 \times 10^{-4}$  m d<sup>-1</sup> which maintains a consistent hydraulic head of approximately 500 m at the northern boundary. The model is discretized into 40 rows and 32 columns where  $\Delta x$  and  $\Delta y$  are both 5 km. Flow is horizontal in the unconfined aquifer and the Dupuit assumptions are maintained. A meandering stream with a path defined by

$$x = \left( \frac{L_x - \Delta x}{2} \right) + 25,000 \text{ m} \sin \left( 2\pi \frac{y - \frac{\Delta y}{2}}{L_y - \Delta y} \right) \quad (2.1)$$

flows from  $y = L_y$  to  $y = 0$ . The width of the streambed,  $w$ , is assumed to be 10 m and the thickness of the streambed sediment,  $b_r$ , is 0.3 m. The channel bottom elevation gradually drops from 453 m at the northern boundary to 45 m at the southern boundary with a constant slope of 0.00204. The hydraulic head of the aquifer also decreases with proximity to the southern boundary to maintain a stream depth of approximately 5 m. Model simulations are run for a 73,000-day (200-yr) period with a time discretization of 160.8 days. A summary of the model parameters is

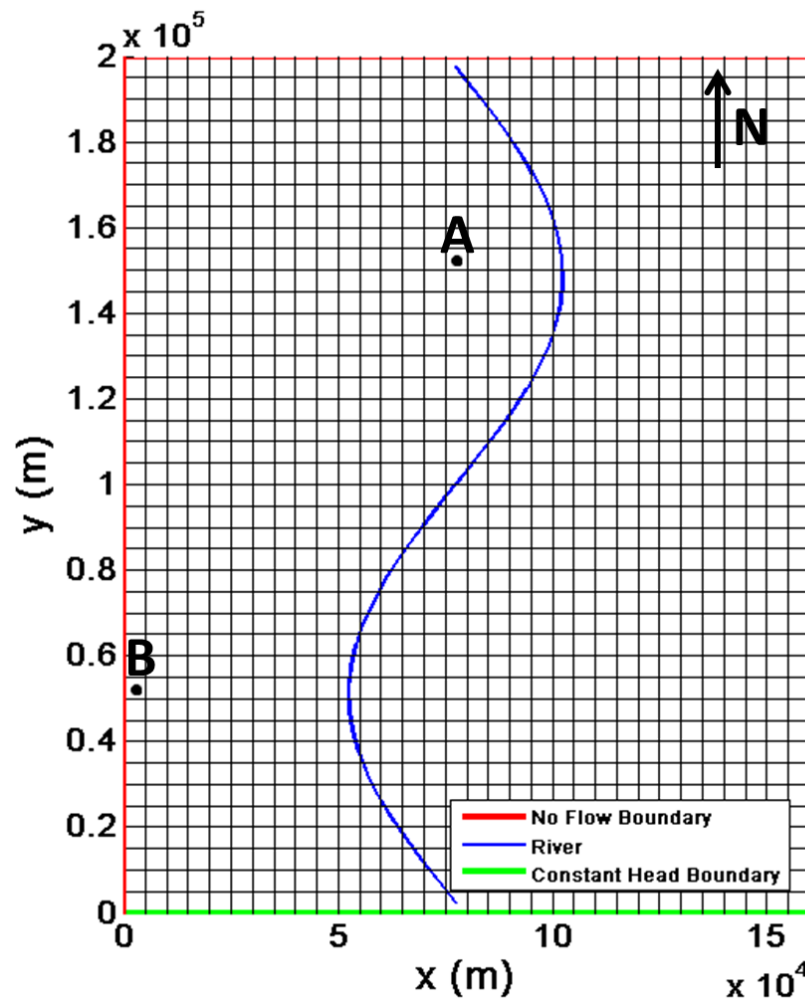


Figure 2.1: Plan view of modeled aquifer with pumping well locations represented at points A  $(x, y) = (77.5 \text{ km}, 152.5 \text{ km})$  and B  $(x, y) = (2.5 \text{ km}, 52.5 \text{ km})$ .

Table 2.1: Model parameters are constant for each of the scenarios investigated in this chapter.

Description	Value
Head at south boundary, at $y = 0$ m	50 m
Elevation of bottom of unconfined aquifer	0 m
Recharge rate, $N$	$6 \times 10^{-4}$ m d <sup>-1</sup>
Stream bottom elevation at north boundary, $z_{rn}$	453 m
Stream bottom at south boundary, $z_{rs}$	45 m
Streambed slope, $S_o$	0.00204
Spectrum of Streambed hydraulic conductivity, $K_r$	$8.64 \times 10^{-5}$ m d <sup>-1</sup> to $8.64 \times 10^2$ m d <sup>-1</sup>
Manning's coefficient of roughness for the Streambed, $n$	0.04
Spatial discretization	50 × 50 km
Temporal discretization	160.8 d
Simulation time, $t_{tot}$	73,000 d
Pumping rate, $Q_p$	10,000 m <sup>3</sup> d <sup>-1</sup>
Specific yield, $S_y$	0.2
Stream width, $w$	10 m
Streambed thickness, $b_r$	0.3 m

provided in Table 2.1.

To investigate the effects of pumping well placement and aquifer  $K$  on stream depletion estimations, we consider the four scenarios listed in Table 2.2. Each scenario assumes either a different location for the pumping well or a different aquifer  $K$ . In all four scenarios, water is extracted from the pumping well at a rate of  $Q_p = 100,000$  m<sup>3</sup> d<sup>-1</sup>. We create 29 variations of each scenario that are identical with the exception of  $K_r$  to assess the sensitivity of the model to this parameter. Each of the model variations is assigned a different homogeneous  $K_r$  within the  $K_r$  spectrum of  $8.64 \times 10^{-1}$  m d<sup>-1</sup> to  $8.64 \times 10^2$  m d<sup>-1</sup>, defined by Calver (2001). The difference between each model streambed  $K_r$  is 0.25 log units. We run model simulations with MODFLOW-2000 and use the block centered flow (BCF) package, the preconditioned conjugate gradient (PCG) solver, and the stream (STR) package.

### 2.3 Equations for Calculating Stream Depletion

In this study, we model the effects of pumping in a multi-dimensional unconfined aquifer with a partially penetrating stream. The hydraulic head in the stream and aquifer are determined

Table 2.2: Model parameters that vary between the scenarios used to investigate the effects of pumping well placement and aquifer  $K$  on stream depletion estimations.

Scenario	Well Location	$K$ (m d <sup>-1</sup> )	Sensitive $K_r$ Range (m d <sup>-1</sup> )
1	A: (77.5 km, 152.5 km)	50	$8.64 \times 10^{-4}$ - $8.64 \times 10^{-2}$
2	B: (2.5 km, 52.5 km)	50	$1.54 \times 10^{-3}$ - $8.64 \times 10^{-2}$
3	A: (77.5 km, 152.5 km)	5	$4.86 \times 10^{-4}$ - $4.86 \times 10^{-2}$
4	A: (77.5 km, 152.5 km)	500	$8.64 \times 10^{-3}$ - $8.64 \times 10^{-1}$

using the governing equation of groundwater flow along with a mass balance on the stream. For this scenario, the governing equation of groundwater flow is

$$S_y \frac{\partial h}{\partial t} = \nabla \cdot [K(h - \zeta)\nabla h] - Q_p \delta(x - x_w)\delta(y - y_w) + N(x, y) - \frac{K_r}{b_r}(h_s - h)B(x, y), \quad (2.2)$$

with initial and boundary conditions of

$$h(x, y, 0) = h_o(x, y) \quad (2.3a)$$

$$h(x, y, t) = 50 \text{ m at } y = 0 \quad (2.3b)$$

$$\nabla h \cdot \mathbf{n} = 0 \text{ at } x = 0, x = 1.6 \times 10^5 \text{ m, and } y = 2 \times 10^5 \text{ m,} \quad (2.3c)$$

where  $S_y$  is the specific yield,  $h$  and  $h_s$  are the hydraulic head in the unconfined aquifer and stream, respectively,  $t$  is time,  $K$  is the hydraulic conductivity of the aquifer,  $\zeta$  is the bottom elevation of the unconfined aquifer,  $(h - \zeta)$  is the saturated thickness of the unconfined aquifer,  $Q_p$  is the rate of pumping,  $\delta$  is the dirac delta function,  $(x, y)$  are spatial coordinates,  $(x_w, y_w)$  are the spatial coordinates of the pumping well,  $N$  is the rate of natural recharge,  $K_r$  and  $b_r$  are the hydraulic conductivity and thickness of the streambed sediments, respectively,  $w$  is the width of the streambed,  $h_o(x)$  is the initial head in the unconfined aquifer,  $\mathbf{n}$  is the outward unit normal vector, and  $B(x, y)$  is a dimensionless parameter that has a value of one at the river and zero everywhere else in the aquifer.

The stream mass balance is defined as

$$\frac{\partial A_{str}}{\partial t} + \frac{\partial Q_{str}}{\partial s} = I/O, \quad (2.4)$$



where  $A_{str}$  is the cross sectional area of the stream is defined,  $Q_{str}$  is the flow rate of the stream,  $s$  is the spatial coordinate along the stream channel defined as positive in the direction of flow (north to south in this work), and  $I/O$  represents inflows and outflows per unit of stream length. We neglect the transient storage term and assume that flow across the streambed ( $Q_s$ ), defined in (1.1), is the only source or sink of water to the stream. This simplifies (2.4) to

$$\frac{\partial Q_{str}}{\partial s} = \frac{wK_r}{b_r} (h_s - h). \quad (2.5)$$

We assume that the cross section of the channel is a wide rectangle and use Manning's equation to approximate  $Q_{str}$ . These assumptions are consistent with the assumptions in the MODFLOW-2000 stream (STR) package.  $Q_{str}$  is defined by

$$Q_{str} = \frac{c}{n} R_h^{2/3} S_o^{1/2} A_{str}, \quad (2.6)$$

where  $c$  is a constant,  $n$  is Manning's roughness coefficient,  $R_h$  is the hydraulic radius, and  $S_o$  is the slope of the channel. The assumption of a rectangular channel allows  $A_{str}$  to be defined as  $w(h_s - z_s)$ , where  $z_s$  is the elevation of the stream channel bottom and  $h_s - z_s$  is depth of the stream. Assuming a channel that is wider than it is long allows  $R_h$  to be approximated as  $h_s - z_s$  and (2.6) can be rewritten as

$$Q_{str} \approx \frac{c}{n} w (h_s - z_s)^{5/3} S_o^{1/2}, \quad (2.7)$$

Combining (2.5) and (2.7) provides

$$\frac{\partial}{\partial s} \left( \frac{c}{n} w (h_s - z_s)^{5/3} S_o^{1/2} \right) = \frac{wK_r}{b_r} (h_s - h) \quad (2.8)$$

We assume the boundary condition of

$$(h_s - z_s) = 0 \text{ at } s = 0 \quad (2.9)$$

for (2.8). The model is set up to create gaining stream conditions, therefore,  $Q_{str}$  is comprised of  $Q_s$  that is contributed along the length of the stream channel.

The initial head distribution,  $h_o$ , was obtained by solving a steady flow simulation using the parameters shown in Table 2.1, with no pumping in the aquifer. The resulting head distribution for the  $K_r = 8.64 \times 10^{-3} \text{ m d}^{-1}$  scenario is shown in Figure 2.2. The hydraulic head in the aquifer, and consequently the saturated thickness, decreases from north to south across the model domain. Viewing the aquifer as a cross sectional in the  $x$  direction would show that hydraulic head is lowest at the location of the stream. This indicates that water from the aquifer is contributing to the stream designating it as a gaining stream. These patterns in hydraulic head are observed for all of the assumed values of streambed  $K_r$ . However, assuming higher and lower  $K_r$  results in a smaller and larger hydraulic head gradients, respectively, in both the  $x$  and  $y$  directions across the model domain.

## 2.4 Results

We solved (2.2) and (2.8) with the boundary and initial conditions in (2.3a), (2.3b), (2.3c), and (2.9), with pumping wells at points A and B in Figure 2.1 using MODFLOW-2000 with the STR package. MODFLOW calculates the flow rate across the stream channel ( $Q_s$ ). To determine the degree to which pumping depleted the stream we found the difference between  $Q_s$  with pumping and  $Q_s$  in the absence of pumping (i.e., the simulation used to generate the initial conditions).

Figure 2.3 shows stream depletion estimation results for the four different scenarios described in Section 2.2. Each set of results in Figure 2.3 shows the degree of stream depletion as a fraction of pumping rate that occurs with time for the 29 different variations of each scenario that assume a different  $K_r$ . The results show that, for each scenario, stream depletion increases at a decreasing rate with time. This trend is observed because of the way in which the cone of hydraulic head depression is formed. When pumping begins, the cone of hydraulic head depression around the well grows rapidly. As the cone expands, the well captures more water that would contribute to stream flow and stream depletion increases. Over time, growth of the cone continues at decreasing rate until the water removed through pumping is equivalent to the water contributed by the surrounding aquifer. Stream depletion continues to increase at a decreasing rate with the formation of the cone

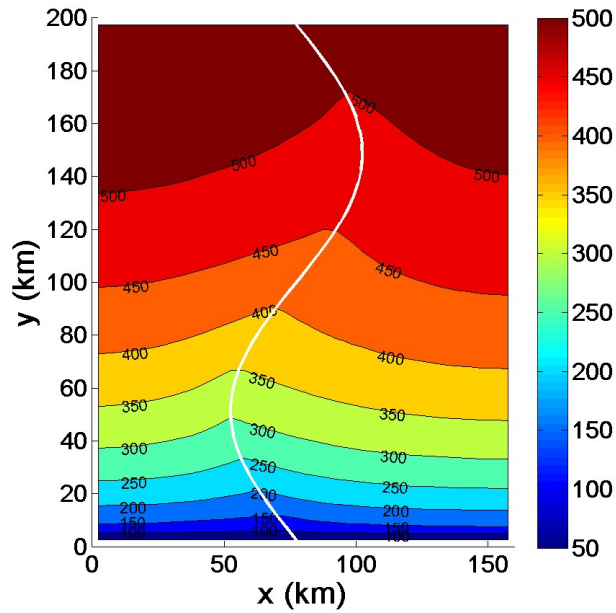


Figure 2.2: Plan view of initial hydraulic head conditions in the modeled aquifer. The stream is represented by a white curve.

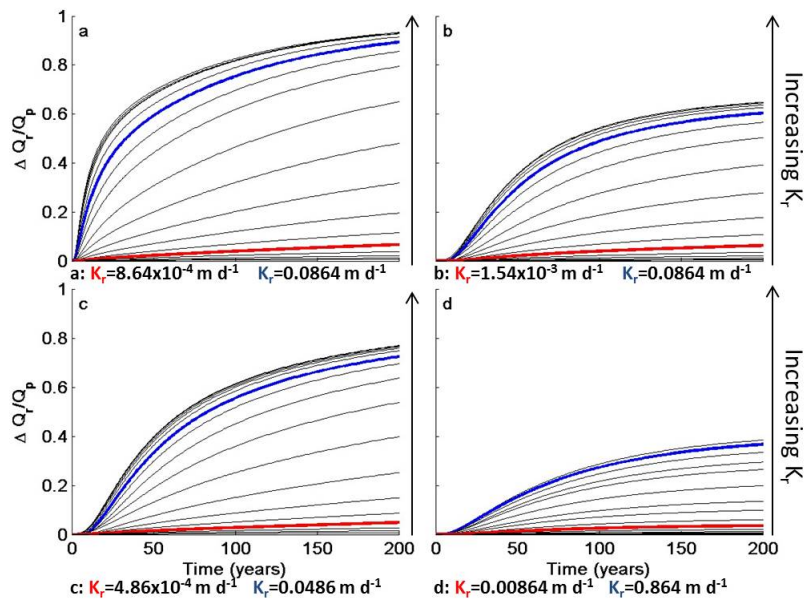


Figure 2.3: Stream depletion as a fraction of pumping rate vs. time for (a) Scenario 1, (b) Scenario 2, (c) Scenario 3, and (d) Scenario 4. Each set of results shows stream depletion estimations for 29 streambeds with a spectrum of  $K_r$  that includes  $8.64 \times 10^{-5}$  (corresponding to lowest stream depletion),  $8.64 \times 10^{-4.75} \dots 8.64 \times 10^2$   $\text{m d}^{-1}$  (corresponding to highest stream depletion). The red and blue curves represent the boundaries of the range of  $K_r$  to which stream depletion estimations are sensitive.

of depression until equilibrium is reached.

In each of the four scenarios considered, model variants assuming a larger  $K_r$  estimated a higher degree of stream depletion than model variants assuming smaller  $K_r$ . For example, in Figure 2.3a, with  $K_r = 8.64 \times 10^{-4} \text{ m d}^{-1}$ , the  $\Delta Q_r/Q_p$  after 200 years is 0.066; and with  $K_r = 8.64 \times 10^{-2} \text{ m d}^{-1}$ , the  $\Delta Q_r/Q_p$  after 200 years is 0.89. This trend is the result of an increased connection between the stream and aquifer. For a losing stream, higher stream-aquifer connectivity leads to an increase in stream depletion because it is easier for a pumping well to draw water across the sediments and out of the stream channel. Gaining streams also experience an increase in stream depletion when the connection between groundwater and surface water is improved. In gaining systems with large streambed conductances, groundwater baseflow more easily contributes to surface flow. Therefore, groundwater pumping, which intercepts baseflow, has the potential to capture more water that would contribute to the flow in the stream and the measured degree of stream depletion increases. From (1.2), note also that an increase in the width of the stream channel ( $w$ ) or the thickness of the streambed sediment ( $b_r$ ) has the same effect on stream depletion as increasing  $K_r$ .

Stream depletion decreases as the distance between the pumping well and the stream increases. The results in Figure 2.3a (pumping at Well A, closer to the stream) and Figure 2.3b (pumping at Well B, farther from the stream) demonstrate this behavior. This trend can be explained by the properties of the cone of hydraulic head depression that forms around the pumping well. The largest drawdown of aquifer hydraulic head occurs in the area immediately surrounding the well. With distance from the well, the aquifer hydraulic head increases and approaches the hydraulic head observed in the nearby aquifer that is not impacted by pumping. Stream depletion occurs when pumping reduces the hydraulic head in the region of the aquifer adjacent to the stream below naturally occurring levels. Therefore, as the pumping well is placed farther from the stream it has less of an impact on the hydraulic head relationship between the aquifer and the stream and the degree of estimated stream depletion is reduced.

Increasing aquifer hydraulic conductivity decreases the degree of stream depletion estimated

at a well location. The results in Figure 2.3c ( $K = 5 \text{ m d}^{-1}$ ) and Figure 2.3d ( $K = 500 \text{ m d}^{-1}$ ) are examples of this trend. These observations are a result of the relationship between aquifer  $K$  and streambed conductance. When aquifer  $K$  is large in comparison to conductance, it is easier for the pumping well to extract water from aquifer storage which reduces the amount of water taken from the stream and reduces the degree of stream depletion. As aquifer  $K$  is decreased in relation to conductance, it is more difficult for the pumping well to draw from aquifer storage. Therefore, it becomes relatively easier for the pumping well to capture water that would contribute to streamflow and stream depletion increases. It should be noted that the results in Figure 2.3a ( $K = 50 \text{ m d}^{-1}$ ) showed greater degree of stream depletion than the results in Figure 2.3c ( $K = 5 \text{ m d}^{-1}$ ). These results are unexpected and have not yet been resolved.

A range of  $K_r$  to which stream depletion estimations are sensitive is observed for each of the scenarios considered. Two insensitive ranges of  $K_r$  exist above and below the upper and lower bounds of the sensitive  $K_r$  range. We determine the sensitivity of a model to a value of  $K_r$  by taking the difference between the  $\Delta Q_r/Q_p$  results from the model with the assumed  $K_r$  of interest and the  $\Delta Q_r/Q_p$  results from two other variations of the model that assume higher and lower  $K_r$  values. We divide each of these differences in  $\Delta Q_r/Q_p$  by the log of their respective changes in  $K_r$ . This relationship is given by

$$\Omega_1 = \frac{\Delta(\Delta Q_r/Q_p)}{\Delta \log K_r}. \quad (2.10)$$

The model is assumed to be sensitive to a specific  $K_r$  when the comparison of the  $K_r$  of interest with higher and lower  $K_r$  scenarios produces  $\Omega_1$  values that are greater than or equal to 0.08. Figure 2.3 and Table 2.2 show the ranges of  $K_r$  to which each of the four scenarios are determined to be sensitive.

Changes in pumping well location and aquifer hydraulic conductivity impact the sensitive  $K_r$  range. Comparing the results in Figure 2.3a (Scenario 1) and Figure 2.3b (Scenario 2) shows that the lower bound of the sensitive  $K_r$  range increases as the pumping well is moved farther away from the stream. Since the upper bound of the sensitive  $K_r$  range is unaffected by the movement

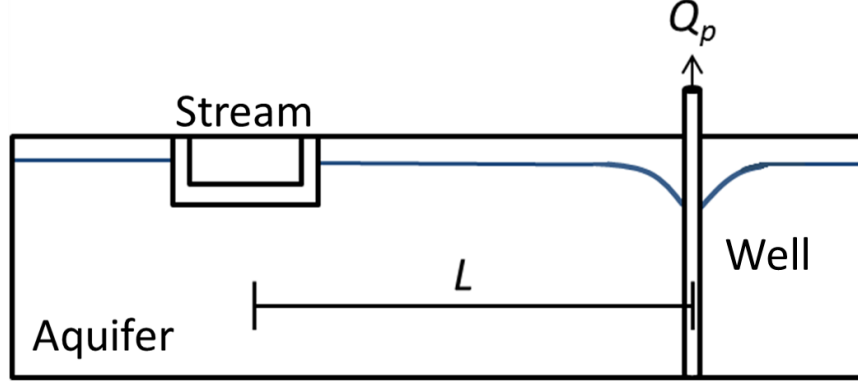


Figure 2.4: Cross sectional view of the assumed hypothetical aquifer in Section 2.5.

of the pumping well, the size of the sensitive  $K_r$  range decreases. Figure 1.2 and Table 1.2 show that the bounds of the sensitive  $K_r$  range increase with the hydraulic conductivity of the aquifer.

## 2.5 Discussion

Our results in Section 2.4 demonstrate that numerical stream depletion estimations are sensitive to a range of  $K_r$  that is characteristic of the model input parameters. In idealistic aquifers, a relationship between the sensitive range of  $K_r$  and the aquifer input parameters can be established. To demonstrate this we consider a homogeneous and isotropic aquifer with a uniform saturated thickness and an infinitely long straight stream at  $x = 0$ . A cross sectional view of this hypothetical aquifer is shown in Figure 2.4. The non dimensional form of the governing equation of groundwater flow for this aquifer can be written as

$$S_y L \frac{\partial h^*}{\partial t} = \frac{Kb}{L} \frac{\partial^2 h^*}{\partial x^{*2}} + \frac{Kb}{L} \frac{\partial^2 h^*}{\partial y^{*2}} - \frac{wK_r}{b_r} (h_s^* - h^*) \delta(x^*) - \frac{Q_p}{L^2} \delta(x^* - 1) \delta(y^*), \quad (2.11)$$

where the definitions of the parameters in Section 2.3 apply and  $h_s^* = h_s/L$ ,  $h^* = h/L$ ,  $x^* = x/L$  and  $y^* = y/L$ . Dividing (2.11) by  $Kb/L$  provides

$$\frac{S_y L^2}{Kb} \frac{\partial h^*}{\partial t} = \frac{\partial^2 h^*}{\partial x^{*2}} + \frac{\partial^2 h^*}{\partial y^{*2}} - \frac{wK_r L}{b_r Kb} (h_s^* - h^*) \delta(x^*) - \frac{Q_p}{KbL} \delta(x^* - 1) \delta(y^*). \quad (2.12)$$

Two dimensionless parameters that govern stream depletion in (2.12) can be identified

$$\Gamma = \frac{Kbt}{S_y L^2} \quad (2.13)$$

$$\Lambda = \frac{wK_r L}{b_r K b}. \quad (2.14)$$

Redefining  $wK_r/b_r$  as streambed conductance ( $C$ ) and  $Kb$  as aquifer transmissivity ( $T$ ), we can rewrite (2.13) and (2.14) as

$$\Gamma = \frac{Tt}{S_y L^2} \quad (2.15)$$

$$\Lambda = \frac{CL}{T}. \quad (2.16)$$

An analytical expression for stream depletion in this system was developed in Hunt (1999) which is described by

$$\frac{\Delta Q_r}{Q_p} = \operatorname{erfc} \left( \sqrt{\frac{1}{4\Gamma}} \right) - \exp \left( \Lambda^2 \Gamma + \frac{\Lambda}{2} \right) \operatorname{erfc} \left( \Lambda \sqrt{\Gamma} + \sqrt{\frac{1}{4\Gamma}} \right). \quad (2.17)$$

Stream depletion estimated by the analytical solution of Hunt (1999) is controlled by  $\Lambda$  and  $\Gamma$ . This means that pumping wells in aquifers with identical values of  $\Lambda$  will cause the same degree of stream depletion when considered as a function of  $\Gamma$ .

Numerical simulations are inherently more complex than analytical solutions. However, the aquifer used in this work, described in Section 2.2, is highly simplified. Consequently, our results in Figure 2.3 suggest that stream depletion may be controlled by  $\Lambda$  and  $\Gamma$ . To investigate the applicability of these dimensionless parameters to our numerical simulations, we use the analytical solution of Hunt (1999) to estimate stream depletion as a function of  $\Gamma$  over a two hundred year period for 29 aquifers with different values of  $\Lambda$ . Similar to our simulations in Section 2.4, each of the 29 scenarios assumes a different  $K_r$  value within the  $K_r$  spectrum of  $8.64 \times 10^{-5} \text{ m d}^{-1}$  to  $8.64 \times 10^2 \text{ m d}^{-1}$ , defined by Calver (2001). A difference of 0.25 log units is assumed between each of the  $K_r$  scenarios. Maintaining the values of  $w$ ,  $L$ ,  $b_r$ , and  $T$  from Scenario 1, described in Tables 2.1 and 2.2, for each of the scenarios creates 29 aquifers with values of  $\Lambda$  that span from  $2.88 \times 10^{-3}$  to  $2.88 \times 10^4$ . The estimations of stream depletion as a function of  $\Gamma$  for these simulations are shown in Figure 2.5.

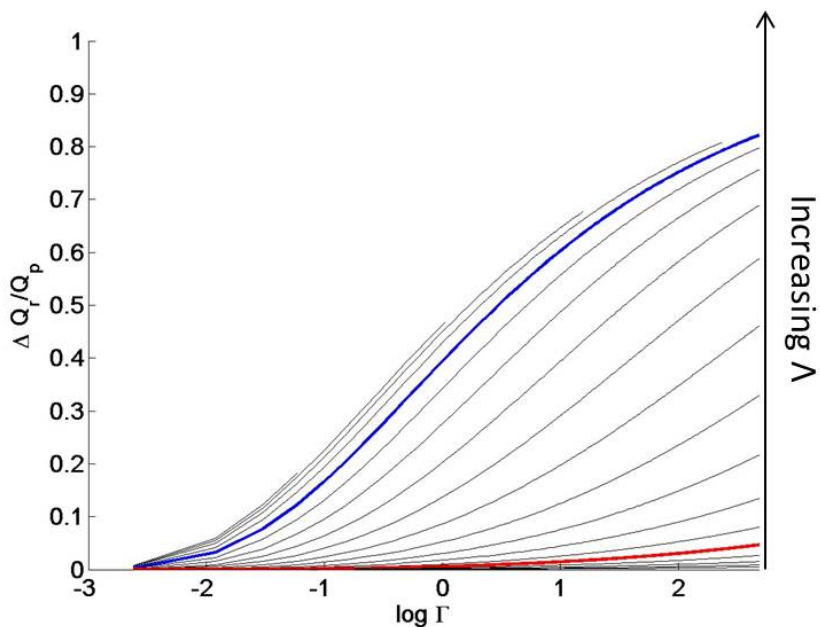


Figure 2.5: Stream depletion vs.  $\log \Gamma$  over a two hundred year period for 29 scenarios with different  $\Lambda$  values determined using the analytical solution of Hunt (1999). The results show stream depletion estimations for 29 aquifers with a spectrum of  $\Lambda$  that spans from  $2.88 \times 10^{-3}$  (corresponding to lowest stream depletion),  $2.88 \times 10^{-2.75}$ ...  $2.88 \times 10^4$  (corresponding to highest stream depletion). The red and blue curves represent the boundaries of the range of  $\Lambda$  to which stream depletion estimations are sensitive.



The results from the analytical solution of Hunt (1999), portrayed in Figure 2.5, show that the degree of stream depletion estimated at a pumping well location increases as the  $\Lambda$  value for the aquifer increases. Considering that  $K_r$  was made larger in each of the increasing  $\Lambda$  scenarios, these results agree with the stream depletion trends observed in Figure 2.3. Also similar to the results in Figure 2.3, a range of  $\Lambda$  exists to which stream depletion estimations are sensitive. We determine the sensitivity of the results from the analytical solution to changes in  $\Lambda$  by altering (2.10). This new parameter used to assess the sensitivity of the analytical solution takes into account variations in  $\Lambda$  and is described as

$$\Omega_2 = \frac{\Delta(\Delta Q_r/Q_p)}{\Delta \log \Lambda}. \quad (2.18)$$

The analytical solution is assumed to be sensitive to a specific value of  $\Lambda$  when the comparison the  $\Lambda$  scenario of interest with higher and lower  $\Lambda$  scenarios produces  $\Omega_2$  values that are greater than or equal to 0.08. For the assumed aquifer, the analytical solution of Hunt (1999) was found to be sensitive to the range of  $\Lambda$  from  $2.88 \times 10^{-2}$  to 9.1 at a time of 200 years. The time at which the sensitivity is assessed for the analytical solution is important because stream depletion estimations for pumping in aquifers that assume small values of  $\Lambda$  eventually increase if estimated over a long enough time period.

We assume the same aquifer input parameters for the analytical estimations of stream depletion in Figure 2.5 and numerical estimations of stream depletion in Figure 2.3a. If the dimensionless numbers  $\Lambda$  and  $\Gamma$  are able to describe the behavior of numerical stream depletion estimations, then the ranges of  $\Lambda$  to which stream depletion estimations are sensitive should be the same between the analytical and numerical solutions. The results for Scenario 1 in Figure 2.3a show that the range of  $K_r$  to which stream depletion estimations are sensitive spans from  $8.64 \times 10^{-4}$  to  $8.64 \times 10^{-2}$  m d<sup>-1</sup>. We use the Scenario 1 aquifer parameters, summarized in Tables 2.1 and 2.2, to determine a sensitive  $\Lambda$  range of  $2.88 \times 10^{-2}$  to 2.88 for the numerical solution.

Comparing the sensitive  $\Lambda$  ranges for the analytical and numerical solutions shows that there is a difference, albeit small, between them. While the uncertainty of the simulations as well as

the imperfections of the sensitivity assessments in (2.10) and (2.18) could be used to argue for the applicability of  $\Lambda$  and  $\Gamma$  to the numerical scenario, they could also be used as arguments against their use. These results demonstrate that even for the simplified aquifer scenario considered in this work, the behavior of numerical stream depletion estimations cannot be predicted with dimensionless numbers. The discrepancy between the sensitive ranges of  $\Lambda$  for the analytical and numerical solutions can be attributed to the increased complexity of the numerical model. Considering that the complexity of numerical models generally increases with applicability, it is likely that  $\Lambda$  and  $\Gamma$  are less applicable to most numerical stream depletion models.

## 2.6 Summary

The results in this chapter show that for every numerical model, ranges of  $K_r$  exist to which stream depletion estimations are sensitive and insensitive. The sensitive and insensitive ranges of  $K_r$  are determined by the by the aquifer properties and the location of the pumping well. Typically, modelers estimating stream depletion assume or calibrate for  $K_r$  which increases the uncertainty of the parameter. In this chapter, we have demonstrated that small variations of  $K_r$  within the sensitive range can significantly impact stream depletion estimations. Therefore, accurately representing  $K_r$  becomes more important if the proposed value is within the sensitive range. We also showed that it is not possible to predict the sensitivity of a model to a value of  $K_r$  using only the model input parameters. These conclusions suggest that a key step in the development of a numerical stream depletion model should be the assessment of the model sensitivity to the proposed value of  $K_r$ .

## Chapter 3

### Effects of Stream Channel Heterogeneity on Stream Depletion: Heterogeneity Along the Stream Channel

#### 3.1 Introduction

With an understanding of the sensitive and insensitive ranges of  $K_r$  in stream depletion estimations, we proceed to investigate how spatial variations of this parameter along the stream channel can affect numerical stream depletion simulations. In Section 3.3 we model the stream channel as a sequence of pools and riffles. We use observed trends of sediment transport behavior to create  $K_r$  heterogeneity patterns that are tied to the flow regime. We investigate the impacts of high and low flow regime  $K_r$  patterns on stream depletion estimations and compare the results to those from two homogeneous  $K_r$  scenarios. The effects of modeling  $K_r$  heterogeneity inside and above the sensitive  $K_r$  range, defined in Chapter 2, are also investigated. In Section 3.4 we model temporal variations in the flow regime by altering between high and low flow  $K_r$  heterogeneity patterns within a single simulation. We consider two scenarios in which the high flow regime occurs either on a half-year or quarter-year basis throughout a one hundred year simulation. We use our results from Sections 3.3 and 3.4 in Section 3.5 to demonstrate the practical implications of spatial and temporal  $K_r$  heterogeneity on the placement of new pumping wells in an aquifer.

In this chapter, we estimate stream depletion as a fraction of the pumping rate ( $\Delta Q_r/Q_p$ ) for all potential pumping well locations in the model domain using the adjoint version of MODFLOW-2000. The adjoint approach calculates stream depletion for a well at every location in the aquifer in a single simulation. Adjoint simulations require some modification to the MODFLOW-2000 input

files and a slightly different version of the stream (STR) package code, which we apply in this study. Griebling (2012) and Griebling and Neupauer (2013) describes the alteration of these input files and the stream (STR) code.

### 3.2 Conceptual Model

We use the hypothetical stream aquifer system portrayed in Figure 2.1 and described in Section 2.1 to create models with spatially and temporally variable streambed  $K_r$ . To establish patterns of  $K_r$  along the stream channel, we assume a sequence of pools and riffles. The stream bends are designated as pools and the straight sections are defined as riffles. Figure 3.1a shows the assumed sequence of pools and riffles along the stream channel. Pools and riffles exhibit different sediment transport behavior based on the flow regime. Under the high flow regime sediments scour from pools and are deposited in riffles; while under the low flow regime the opposite behavior is observed (Clayton and Pitlick, 2007). The sections of the stream channel that are scouring and filling can be represented as regions of high  $K_r$  and low  $K_r$ , respectively. Thus, high and low flow conditions create different patterns of streambed  $K_r$ .

To model the streambed under the high flow regime, we vary  $K_r$  linearly over two orders of magnitude along the stream channel between a high  $K_r$  at the point of maximum curvature and a low  $K_r$  at the point of minimum curvature. The  $K_r$  pattern is reversed for the low flow regime resulting in a high  $K_r$  at the minimum point of curvature that is two orders of magnitude larger than the low  $K_r$  at the maximum point of curvature. Figure 3.1b and Figure 3.1c show the patterns of high and low  $K_r$  along the stream channel for the high and low flow regimes, respectively.

### 3.3 Effects of River Flow Regime on Stream Depletion

In this section, we investigate how patterns of  $K_r$  heterogeneity for the high and low flow regime impact stream depletion estimations. A mean  $K_r$  of  $8.64 \times 10^{-3} \text{ m d}^{-1}$ , in the center of the sensitive  $K_r$  range defined in Chapter 2, is maintained for the heterogeneous scenarios. We model linear variations of  $K_r$  over two orders of magnitude from a low  $K_r$  value of  $1.71 \times 10^{-4} \text{ m d}^{-1}$  to a

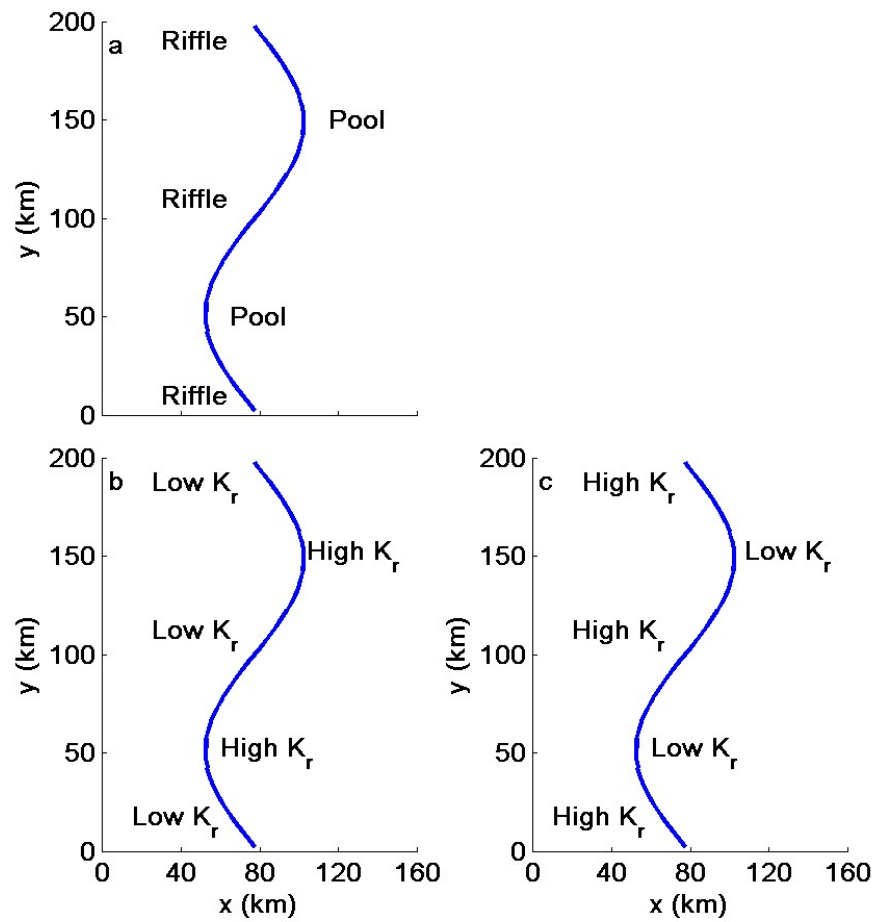


Figure 3.1: Plan view of the modeled aquifer showing (a) the assumed pool and riffle sequence (b) the streambed  $K_r$  pattern under high flow regime conditions and (c) the streambed  $K_r$  pattern under low flow regime conditions.

high  $K_r$  value of  $1.71 \times 10^{-2} \text{ m d}^{-1}$  for the high and low flow regime scenarios in accordance with the  $K_r$  patterns established in Figure 3.1. For comparison, we perform stream depletion estimations for two homogeneous scenarios in which we assume the maximum  $K_r$  ( $1.71 \times 10^{-2} \text{ m d}^{-1}$ ) and average  $K_r$  ( $8.64 \times 10^{-3} \text{ m d}^{-1}$ ) from the heterogeneous simulations. We investigate the significance of modeling variations of  $K_r$  above of the sensitive range by estimating stream depletion for high and low flow regime scenarios that assume a mean  $K_r$  of  $8.64 \times 10^{-1} \text{ m d}^{-1}$ . For these models,  $K_r$  varies linearly from a minimum of  $1.71 \times 10^{-2} \text{ m d}^{-1}$  to a maximum of  $1.71 \text{ m d}^{-1}$ .

The results in Figure 3.2 and Figure 3.3 summarize calculations of  $\Delta Q_r/Q_p$  at every potential well location in the model domain for the high flow, low flow, homogeneous and insensitive scenarios. The scale of  $\Delta Q_r/Q_p$  is the same for the results in Figure 3.2; however, the  $\Delta Q_r/Q_p$  scale changes for the insensitive scenario results in Figure 3.3 because of the larger mean  $K_r$  assumed in these models. In all of the cases we consider,  $\Delta Q_r/Q_p$  increases with proximity of the pumping well location to the stream. This trend is observed because the pumping well captures more water that would otherwise contribute to stream flow as it is moved closer to the stream. Similarly, as a pumping well is placed further away from the stream, it captures a greater amount of water that would otherwise not contribute to stream flow and a lesser degree of  $\Delta Q_r/Q_p$  is calculated. This relationship between the percentage of water captured that would contribute to stream flow and the percentage of water captured that would not contribute to stream flow is what dictates the degree of  $\Delta Q_r/Q_p$  calculated at a potential well location. Changes to the physical system, e.g. the model  $K_r$ , can alter this relationship and impact the degree of  $\Delta Q_r/Q_p$  estimated throughout the model domain. The model boundary conditions can also affect the calculation of  $\Delta Q_r/Q_p$  at a well location. In all of the scenarios considered, a constant head boundary is set at the southern end of the model domain. Stream depletion estimations decrease near this boundary because pumping wells located in this region pull water across the boundary instead of capturing water that would contribute to stream flow.

The influence of the modeled  $K_r$  heterogeneity patterns are visible in the estimations of  $\Delta Q_r/Q_p$  for the high flow (Figure 3.2a) and low flow (Figure 3.2b) regime scenarios. Increases

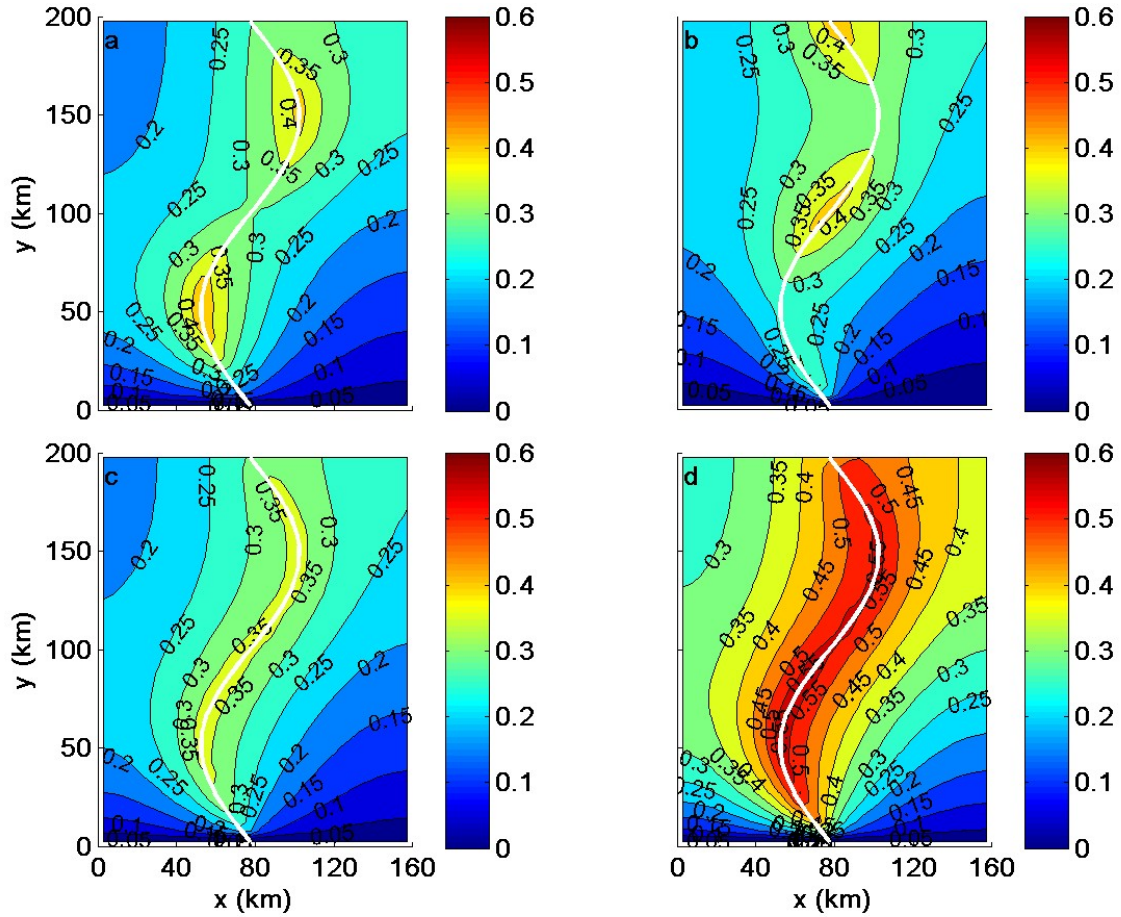


Figure 3.2: Stream depletion calculated as a fraction of pumping rate ( $\Delta Q_r/Q_p$ ) at each potential well location in the model domain for (a) a heterogeneous stream channel with high flow regime  $K_r$  patterns (b) a heterogeneous stream channel with low flow regime  $K_r$  patterns (c) a homogeneous stream channel with an assumed  $K_r$  equivalent to the mean  $K_r$  from the heterogeneous scenarios and (d) a homogeneous stream channel with an assumed  $K_r$  equivalent to the maximum  $K_r$  from the heterogeneous scenarios. A mean  $K_r$  of  $8.64 \times 10^{-3} \text{ m d}^{-1}$  is assumed for a, b and c and a  $K_r$  of  $1.71 \times 10^{-2} \text{ m d}^{-1}$  is assumed for d.

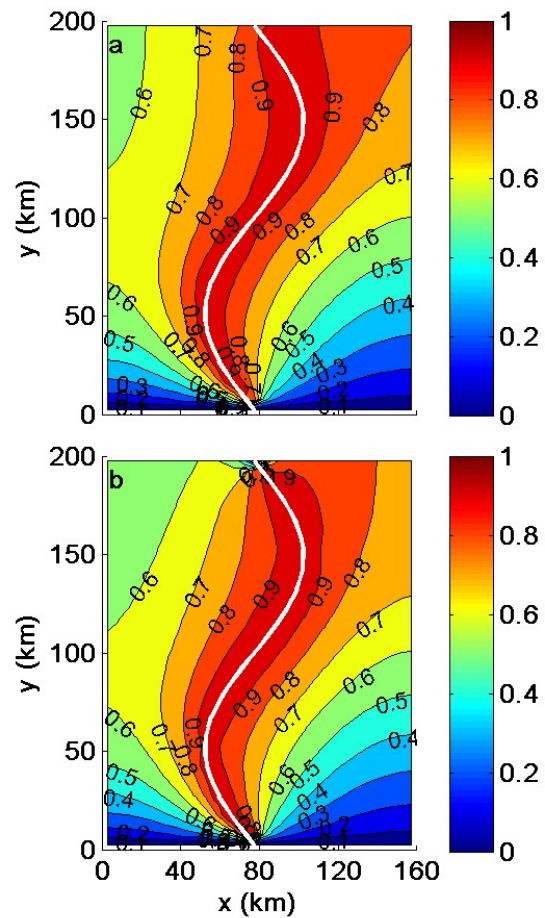


Figure 3.3: Stream depletion calculated as a fraction of the pumping rate ( $\Delta Q_r/Q_p$ ) at each potential well location in the model domain for patterns of  $K_r$  heterogeneity that represent the (a) high and (b) low flow regime. A mean  $K_r$  of  $8.64 \times 10^{-1} \text{ m d}^{-1}$ , above the sensitive range defined in Chapter 2, is assumed for the simulations.



in  $K_r$  improve the hydraulic connection between the aquifer and the stream. A better connection makes it easier for a pumping well along a high  $K_r$  reach to capture water that would otherwise contribute to stream flow, which increases the degree to which the stream is depleted. Decreases in  $K_r$  reduce the stream-aquifer connection and make it harder for nearby pumping wells to impact stream flows, which reduces stream depletion. For each simulation, a greater degree of  $\Delta Q_r/Q_p$  is estimated for pumping well locations near sections of the stream channel modeled with high  $K_r$ . Conversely, a lesser degree of  $\Delta Q_r/Q_p$  is estimated for well locations near regions of low  $K_r$ . Thus, a trend of increasing  $\Delta Q_r/Q_p$  for pumping along the stream bends and decreasing  $\Delta Q_r/Q_p$  for pumping along the straight sections of the stream is observed in the results for the high flow regime scenario (Figure 3.2a). These spatial trends of high and low  $\Delta Q_r/Q_p$  are reversed for the results from the low flow regime scenario (Figure 3.2b), because of the reversal of the  $K_r$  heterogeneity pattern.

The results from both of the homogeneous scenarios (Figure 3.2c and Figure 3.2d) show a decrease in  $\Delta Q_r/Q_p$  with distance from the stream channel that is independent of the position along the stream channel. This effect permeates into the surrounding aquifer as the pattern of decreasing  $\Delta Q_r/Q_p$  resembles the shape of the stream channel. The value of  $K_r$  assumed for the homogeneous stream channel greatly impacted stream depletion results. Stream depletion estimations were larger for an aquifer with a homogeneous  $K_r$  near the upper end of the sensitive  $K_r$  spectrum (Figure 3.2d) than they were for an aquifer with a homogeneous  $K_r$  near the middle of the sensitive  $K_r$  spectrum (Figure 3.2c).

Modeling  $K_r$  heterogeneity, when the mean  $K_r$  is above the sensitive range, is shown to be insignificant by the results from the insensitive scenarios (Figure 3.3). In the insensitive models, patterns of  $K_r$  heterogeneity for the high and low flow regime are assumed with a mean  $K_r$  above the sensitive range. While the results from the high (Figure 3.2a) and low (Figure 3.2b) flow regime scenarios show patterns of  $\Delta Q_r/Q_p$  that correspond with the modeled variations in  $K_r$  along the stream channel, the insensitive scenarios (Figure 3.3) do not. Therefore, while not identical, the  $\Delta Q_r/Q_p$  results from the insensitive high flow (Figure 3.3a) and insensitive low flow

(Figure 3.3b) simulations are similar. The patterns of  $\Delta Q_r/Q_p$  produced with the insensitive scenarios more closely resemble the the patterns observed in the results from the homogeneous simulations(Figure 3.2c and Figure 3.2d). A constant degree of  $\Delta Q_r/Q_p$  is estimated along the length of the stream channel and no increase or decrease is observed at the stream bends or straight sections. These results suggest that it is only significant to account for  $K_r$  heterogeneity when stream depletion estimations are sensitive to the mean  $K_r$  of the modeled stream channel.

The results in Figure 3.2 and Figure 3.3 emphasize the importance of understanding the sensitivity of a numerical stream depletion model to the assumed value of  $K_r$ . If  $K_r$  is within the sensitive range, natural  $K_r$  variations have the potential to alter the distribution of  $\Delta Q_r/Q_p$  estimated throughout the model domain. This can be seen in the heterogeneous results in Figure 3.2a and Figure 3.2b as well as the homogeneous results in Figure 3.2c and Figure 3.2d. The heterogeneous results show that  $K_r$  variations along the stream within the channel with  $K_r$  in the sensitive rang can alter the pattern of  $\Delta Q_r/Q_p$  estimated for pumping well locations in the region around the stream. The homogeneous results demonstrate how a change in the assumed  $K_r$  within the sensitive range can increase  $\Delta Q_r/Q_p$  estimations throughout the entire model domain.

### 3.4 Effects of a Temporally Variable River Flow Regime on Stream Depletion

In this section, we simulate the effects of temporally variable  $K_r$  on stream depletion estimations over a one hundred year period. We use our previously established patterns of  $K_r$  heterogeneity for the high and low flow regime, described in Sections 3.2 and 3.3, to investigate two scenarios in which the flow regime is altered over different time intervals throughout the simulation. In the first scenario (Scenario 1) we model variations between the high and low flow regime on a half-year basis and assume that the flow regimes occur for equivalent time periods. The time intervals for the flow regimes are adjusted in the second scenario to investigate the impacts of a quarter-year occurrence of the high flow regime. Thus, in the second scenario (Scenario 2), the high and low flow regimes are modeled for 25% and 75% of the overall simulation time, respectively. Table 3.1 summarizes the temporal setup of the models used in Scenarios 1 and 2.

Table 3.1: Temporal setup of the two models used in Scenarios 1 and 2 that investigate the impacts of the high flow regime occurring for one half and one quarter of the year, respectively.

Description	Scenario 1	Scenario 2
Model simulation time	36525 d	36525 d
Number of transient stress periods	200	200
Length of high flow stress periods	182.625 d	91.3125 d
Length of low flow stress periods	182.625 d	273.9375 d
$\Delta t$	18.2625 d	10.15 d

In both temporal scenarios, the modeled aquifer quickly responds to changes in the  $K_r$  heterogeneity pattern. This results in fluctuations of calculated  $\Delta Q_r/Q_p$  with time that occur independently of the length of the high flow regime stress period. Figure 3.4 shows the temporal oscillations of  $\Delta Q_r/Q_p$  for a scenario that assumes a half-year high flow regime calculated for a pumping well located directly on top of a stream bend at  $(x,y)=(77.5 \text{ km}, 102.5 \text{ km})$ . Due to the location of the well,  $\Delta Q_r/Q_p$  increases during the stress periods that assume patterns of  $K_r$  representative of the high flow regime and decreases during the stress periods that assume patterns of  $K_r$  for the low flow regime. The difference between the maximum and minimum  $\Delta Q_r/Q_p$  observed during the stress periods that assume the high and low flow regimes increases over the first twenty years of the simulation and then reaches a steady state for the rest of the one hundred year period. The mean of the  $\Delta Q_r/Q_p$  oscillations increases with time and exhibits the behavior of a  $\Delta Q_r/Q_p$  versus time curve produced with a model that does not assume temporal variations in  $K_r$ .

As a result of the rapid response of the model to temporal variations in  $K_r$ , spatial distributions of  $\Delta Q_r/Q_p$  determined at the end of a stress period are characteristic of  $K_r$  pattern assumed for the flow regime in that period. The results in Figure 3.5 and Figure 3.6 demonstrate this behavior by showing calculations of  $\Delta Q_r/Q_p$  at every potential pumping well location in the model domain for the last two stress periods of the simulations that vary the high flow regime over half and quarter-year intervals, respectively.

Figure 3.5a and Figure 3.6a show the spatial distribution of  $\Delta Q_r/Q_p$  estimated for the half

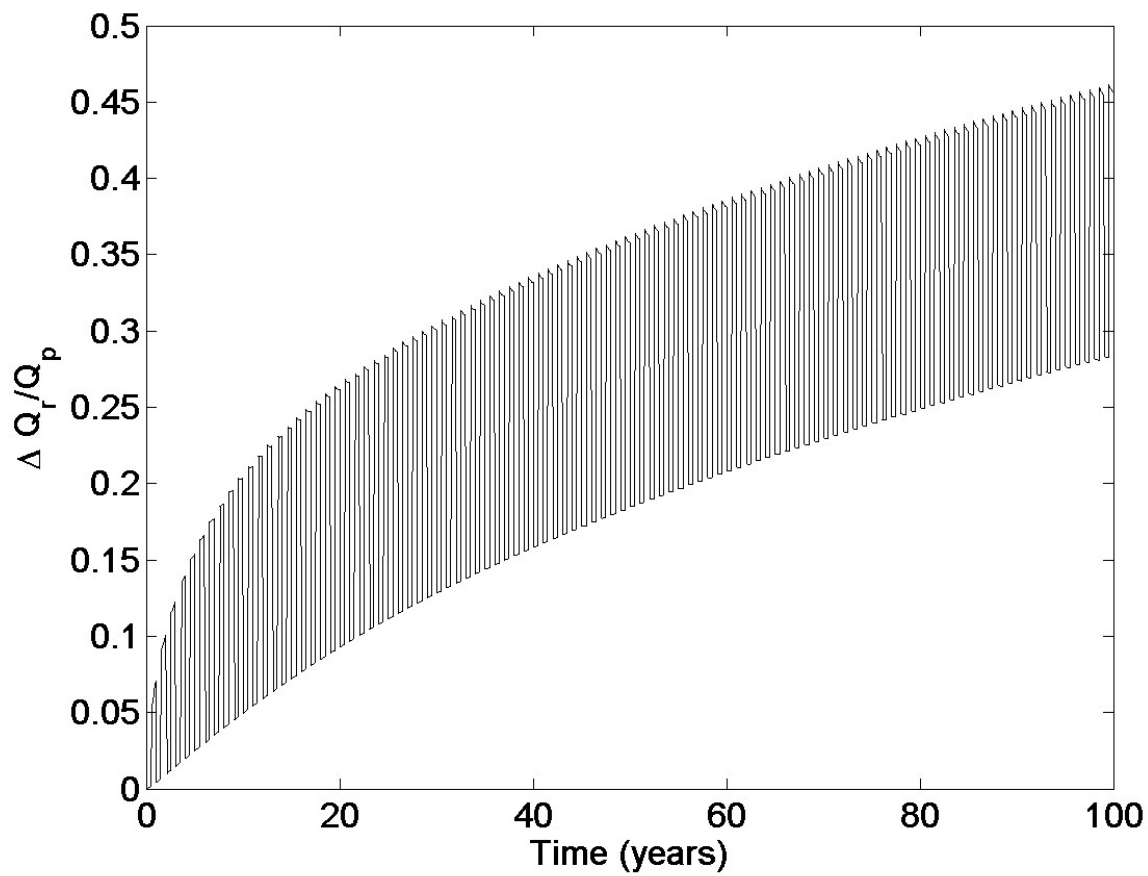


Figure 3.4: Stream depletion as a fraction of the pumping rate ( $\Delta Q_r/Q_p$ ) vs. time due to a pumping well located at  $(x,y)=(77.5 \text{ km}, 102.5 \text{ km})$  in the model domain. Results are representative of the temporally variable half-year high flow scenario.

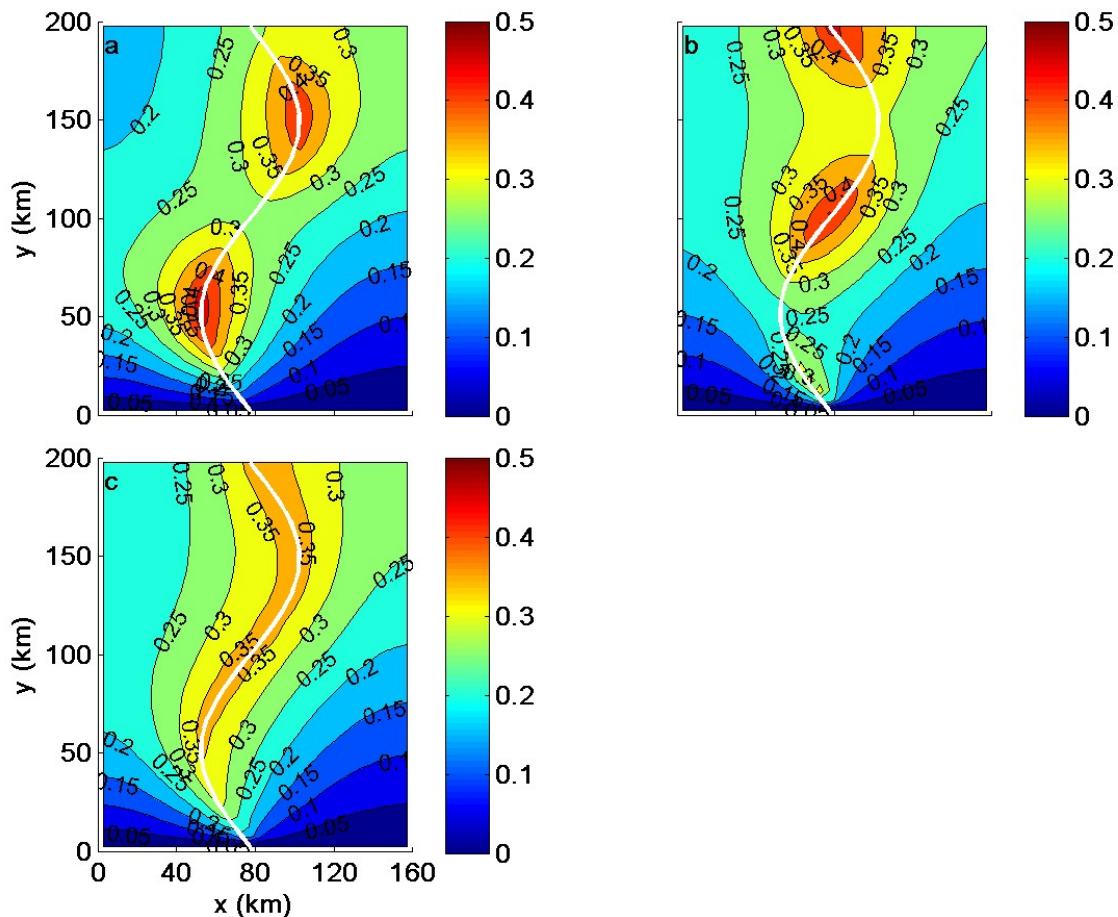


Figure 3.5: Stream depletion calculated as a fraction of the pumping rate for each potential well location in the model domain for the scenario in which the high flow regime is varied over half-year intervals. Stream depletion results from the the end of the second to last stress period and the end of the last stress period are shown in (a) and (b), respectively. The average of the results in (a) and (b) are shown in (c).

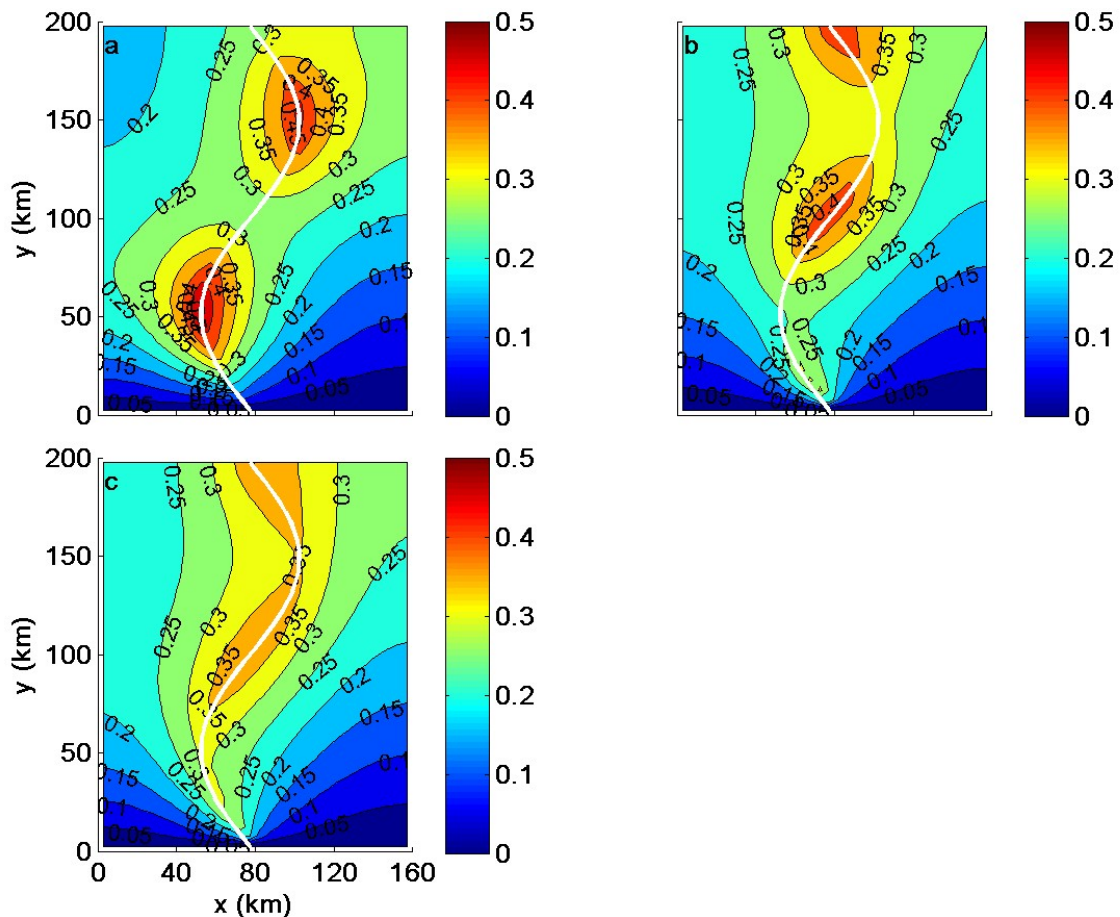


Figure 3.6: Stream depletion calculated as a fraction of the pumping rate for each potential well location in the model domain for the scenario in which the high flow regime is assumed for one quarter of the year. Stream depletion results from the the end of the second to last stress period and the end of the last stress period are shown in (a) and (b), respectively. The weighted average of the results in (a) and (b) are shown in (c).

and quarter-year scenarios at the end of the second to last stress period. The pattern of  $K_r$  heterogeneity for the high flow regime was assumed for this stress period. Consequently, the stream depletion patterns for both temporal scenarios resemble the results shown in Figure 3.2a from the scenario in which the pattern of  $K_r$  heterogeneity for the high flow regime is assumed to be constant with time. In the final stress period of the temporal simulations, the flow regimes are switched from high to low flow and the  $K_r$  heterogeneity patterns are modeled accordingly. Figure 3.5b and Figure 3.6b show the distribution of  $\Delta Q_r/Q_p$  in the model domain at the end of the final stress period for each temporal simulation. The resulting patterns of stream depletion resemble the patterns observed in Figure 3.2b from the scenario in which a low flow pattern of  $K_r$  heterogeneity is assumed to be constant with time.

We average the estimations of  $\Delta Q_r/Q_p$  from the final two stress periods for the half and quarter-year temporally variable  $K_r$  scenarios in Figure 3.5c and Figure 3.6c, respectively. A weighted average is used for the quarter-year scenario to account for the difference between the length of the stress periods in which the patterns of  $K_r$  heterogeneity for the high and low flow regime are assumed. The averaged results from the half-year high flow scenario resemble the results from the homogeneous  $K_r$  scenario shown in Figure 3.2c. The pattern of  $\Delta Q_r/Q_p$  observed throughout the model domain for the averaged quarter-year results is different because of the dominance of low flow conditions in the simulation. Thus, the degree of  $\Delta Q_r/Q_p$  calculated for pumping well locations along the straight sections of the stream channel is slightly larger than the degree of  $\Delta Q_r/Q_p$  estimated for pumping well locations near the stream bends.

The results from the temporally variable  $K_r$  scenario demonstrate that, for the situations investigated in this study, the aquifer responds quickly to alterations in streambed  $K_r$ . This immediate response time causes the estimations of  $\Delta Q_r/Q_p$  to reflect the patterns of  $K_r$  heterogeneity assumed for the stress period in which  $\Delta Q_r/Q_p$  is calculated. Thus, estimating  $\Delta Q_r/Q_p$  at the end of any single stress period will produce results that resemble the simulations from scenarios in which  $K_r$  is assumed to be non temporally variable. Therefore, the  $\Delta Q_r/Q_p$  results from two stress periods must be averaged to produce a distribution of  $\Delta Q_r/Q_p$  that is influenced by two separate

$K_r$  heterogeneity patterns.

### 3.5 Practical Implications

It is often the case that legal or environmental restrictions limit the feasibility of pumping well locations in a region. Thus, numerical estimations of stream depletion are typically used to aid the placement of new pumping wells in an aquifer. In this section, we investigate how accounting for spatial and temporal variations in  $K_r$  affect the feasibility of pumping well locations. We compare the  $\Delta Q_r/Q_p$  results from the simulations described in Sections 3.3 and 3.4 with the results from the homogeneous  $K_r$  scenario shown in Figure 3.2c. We use this homogeneous scenario as a basis for comparison because it is currently standard practice for modelers estimating stream depletion to assume or calibrate for a homogeneous model  $K_r$ . Therefore, through comparison with a homogeneous base case we demonstrate how the assumption of different  $K_r$  heterogeneity patterns impact the estimation of feasible pumping well locations in a model domain.

For each scenario, we assume that a pumping well can be placed at any location where  $\Delta Q_r/Q_p$  is calculated to be less than 0.3. We compare the affects of different  $K_r$  heterogeneity patterns on the feasibility of pumping well locations in model domain by superimposing the calculated 0.3  $\Delta Q_r/Q_p$  contour from different simulations onto the results from the homogeneous base case. Comparing the difference between the imposed 0.3  $\Delta Q_r/Q_p$  contour and the 0.3  $\Delta Q_r/Q_p$  contour from the base scenario highlights the regions of the models where the feasibility of pumping changes.

In Figure 3.7 the  $\Delta Q_r/Q_p$  results from the high flow, low flow, high  $K_r$  homogeneous and insensitive scenarios described in Section 3.3 are compared with the homogeneous base case. The impact of the  $K_r$  heterogeneity patterns assumed for the high and low flow scenarios are shown in Figure 3.7a and Figure 3.7b, respectively. In both scenarios, regions of increased and decreased  $K_r$  along the stream channel alter the feasibility of pumping well locations along the stream channel. Under the high flow regime, the increased  $K_r$  along the stream bends results in a larger range of infeasible pumping well locations than what is observed in the base case. The feasibility of pumping



well locations along the straight section of the stream increases due to the decrease in model  $K_r$ . Under the low flow regime, the  $K_r$  heterogeneity pattern is reversed. Thus, the feasibility of pumping well locations decreases along the straight sections of the stream and increases along the stream bends.

Comparisons of the base case with the high  $K_r$  homogeneous scenario, in Figure 3.2d, and the insensitive scenarios, in Figure 3.3, are shown in Figure 3.7c and Figure 3.7d. The  $K_r$  assumed for the high  $K_r$  homogeneous scenario is the maximum  $K_r$  modeled in the high and low flow regime scenarios. This increase in  $K_r$  along the entire length of the stream channel decreases the feasibility of pumping well locations throughout the entire aquifer and pushes the region of feasible well locations away from the stream in a shape that resembles the stream channel. The insensitive scenarios assume a mean  $K_r$  that is even larger than the maximum  $K_r$  used in the heterogeneous scenarios. As a result the majority of pumping well locations in the model domain become infeasible with the exception of the locations influenced by the southern head boundary.

The effects of temporal variations in  $K_r$  heterogeneity are demonstrated in Figure 3.8. The half-year fluctuations between high and low flow  $K_r$  patterns, shown in Figure 3.8a, slightly reduce the feasibility of pumping well locations along the length of the stream channel. A greater impact on pumping well feasibility is observed in Figure 3.8b, which compares the base case with a quarter-year high flow temporally variable  $K_r$  scenario. The decreased feasibility of pumping along the straight sections of the stream is a result of more pronounced affects of the low flow conditions on the  $\Delta Q_r/Q_p$  estimations in the model aquifer.

### 3.6 Summary

The significance of modeling the different  $K_r$  patterns discussed in this chapter can be gleaned from the results in Figure 3.7 and Figure 3.8. For example, the comparison of the results from the scenarios assuming patterns of  $K_r$  heterogeneity for the high and low flow regime with the results from the base case in Figure 3.7a and Figure 3.7b show that, if the assumed mean  $K_r$  of the model is in the sensitive range,  $K_r$  variations along the stream channel can impact the feasibility of pumping

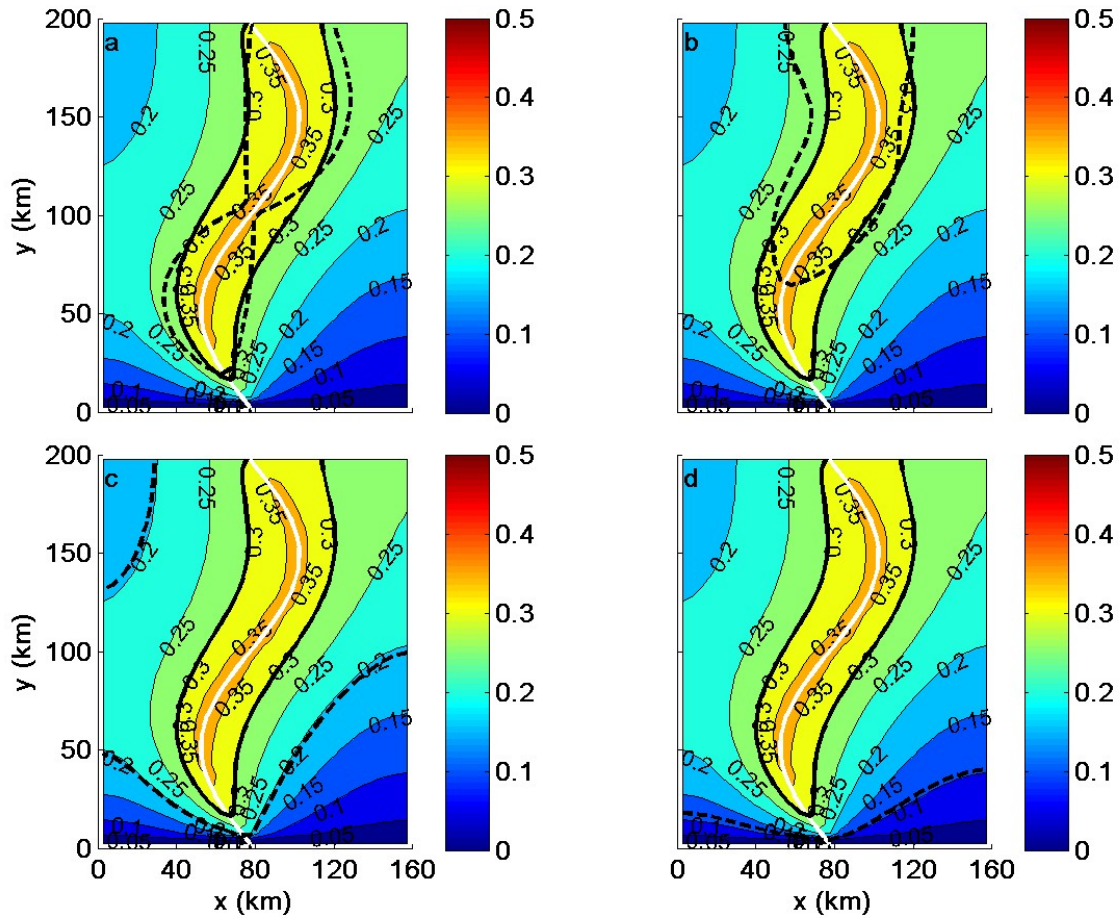


Figure 3.7: Comparison of the feasible pumping well locations in a homogeneous base case scenario with (a) a scenario in which patterns of  $K_r$  heterogeneity for the high flow regime are assumed (b) a scenario in which patterns of  $K_r$  heterogeneity for the low flow regime are assumed (c) a scenario that assumed a homogeneous stream channel with higher  $K_r$  (d) an insensitive scenario. The  $0.3 \Delta Q_r/Q_p$  contour from the homogeneous base scenario is emphasized as a thick black line. The superimposed  $0.3 \Delta Q_r/Q_p$  contour is represented as a thick black dashed line.

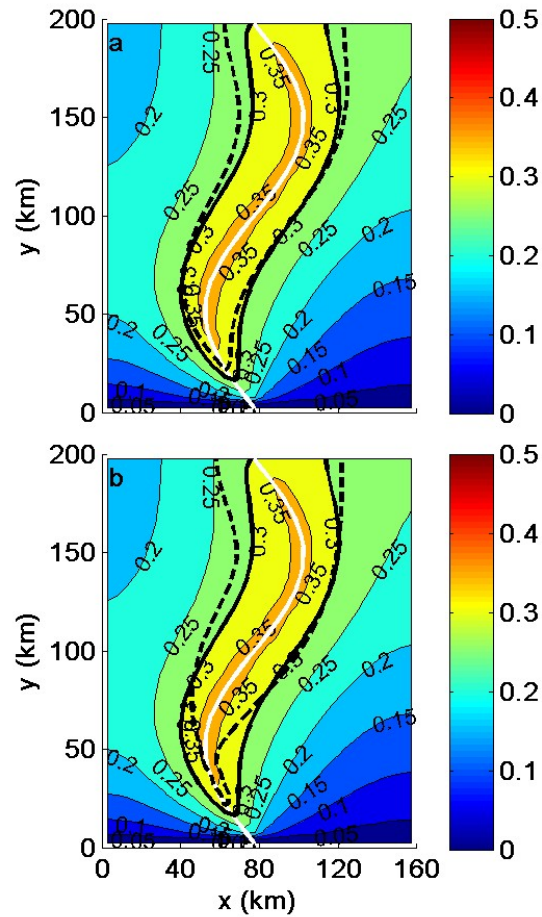


Figure 3.8: Comparison of the feasible pumping well locations in a homogeneous base case scenario with a (a) half-year high flow temporally variable  $K_r$  scenario and (b) quarter-year high flow temporally variable  $K_r$  scenario. The 0.3  $\Delta Q_r/Q_p$  contour from the homogeneous base scenario is emphasized as a thick black line. The superimposed 0.3  $\Delta Q_r/Q_p$  contour from the comparison scenario is represented as a thick black dashed line.

well locations surrounding the stream. However, Figure 3.8 shows that temporal variations of these high and low flow regime  $K_r$  patterns lessens the impact of these assumptions on pumping well feasibility. The  $K_r$  modeling schemes that had the greatest impact on the feasibility of pumping well locations in the aquifer were the high  $K_r$  homogeneous and insensitive scenarios. The comparison of these results with the base case emphasize how variations of  $K_r$  within and beyond the sensitive  $K_r$  range can significantly impact stream depletion estimations.

## Chapter 4

### Discussion, Conclusions and Future Work

In this final chapter, we discuss the assumptions and limitations of our work. We summarize our conclusions and discuss areas where our work on understanding the effects of modeling  $K_r$  heterogeneity in stream depletion estimations could be furthered.

#### 4.1 Assumptions

To investigate the sensitivity of numerical stream depletion estimations to  $K_r$  and understand the significance of modeling streambed heterogeneity, we make several assumptions. In our model, we assume that the Dupuit assumption holds and flow is horizontal in our unconfined aquifer. We also assume a one layer, homogeneous, isotropic and unconfined aquifer. This simplified scenario is considered in order to clearly understand the effects of varying  $K_r$  on stream depletion estimations.

#### 4.2 Limitations

Our work is a simplified demonstration of the sensitivity of numerical stream depletion estimations to model  $K_r$ . We seek to impact current stream depletion estimation practices by focusing our investigation on how  $K_r$  variations affect simulations performed using the widely applied program MODFLOW-2000. However, MODFLOW-2000 is limited in its ability to model interactions between surface water and groundwater.

The conceptualization behind MODFLOW-2000 impairs the ability of the program to simulate key aspects of the flow between surface water and groundwater. Brunner (2010) highlights the

shortcomings of the program by citing the following assumptions made in all of the MODFLOW stream simulation packages .

1. Negative pressure gradients are unaccounted for in the unsaturated zone. This leads to an underestimation of infiltration flux across the bed of streams that are disconnected from the water table.

2. Each consecutive cell, to which the properties of the stream are assigned, is assumed to be downstream of the previous cell. As a result, assigning the stream to two adjacent grid cells that are perpendicular to flow simulates an abrupt shift in the flow direction instead of a wider stream channel. Thus, the determination of the connection between the stream and the underlying water table is done on a cell by cell basis. Streams are determined to be either connected or disconnected from the water table over expanses of the stream determined by the model discretization.

3. Often, a discrepancy exists between the width of the modeled stream and the discretization of the model grid. This leads to errors because the exchange rates between surface water and groundwater are distributed over the entire area of the grid cell instead of the area of the stream.

4. MODFLOW-2000 models are often coarsely discretized in the vertical direction to avoid aquifer cells going dry. This results in the assumption that hydraulic head does not vary in the vertical direction which is often not the case for scenarios in which stream flow infiltrates into the underlying aquifer.

This work is further limited by our use of the stream (STR) package for stream flow simulation in MODFLOW-2000. The package assumes that the stream channel has a wide rectangular geometry where the flow depth is much smaller than the width of the channel. However, streams typically have variable channel geometries that cannot be represented with a rectangle.

The STR package and MODFLOW-2000 also limit the degree to which streambed heterogeneity can be modeled. Streambed hydraulic properties, such as  $K_r$ , are designated on a cell by cell basis. Because the stream is simulated in consecutive downstream model grid cells, the assigned properties define sections of the stream that are determined by the model discretization. Thus, it is impossible to model complex streambed heterogeneity in coarsely discretized models. It is also

impossible to model streambed heterogeneity across the stream channel for a single stream. For these reasons, we modeled patterns in  $K_r$  heterogeneity along the length of the stream channel.

### 4.3 Conclusions

This work proves that numerical stream depletion estimations are sensitive and insensitive to ranges of  $K_r$ . The sensitive  $K_r$  range is dependent on the aquifer properties. If a modeler assumes or calibrates for a  $K_r$  that is within the sensitive range, a slight variation in the assigned value could significantly alter the resulting stream depletion estimations. Considering the uncertainty that is introduced from the assumption or calibration of a parameter, the assessment of the model sensitivity to the proposed value of  $K_r$  should be an essential step in the development of a numerical stream depletion model.

Natural stream channels are highly heterogeneous and typically have  $K_r$  values that vary over several orders of magnitude. The significance of accounting for this  $K_r$  heterogeneity in numerical stream depletion estimations is also investigated in this work. We apply concepts from stream channel geomorphology to develop patterns of  $K_r$  heterogeneity along the stream channel for high and low flow conditions. Our results show that varying  $K_r$  over the sensitive range along the stream channel can significantly impact the degree of stream depletion estimated for nearby pumping well locations.

We develop a method for assessing the impact of temporally variable streambed heterogeneity patterns on stream depletion estimations. We simulate changes between the high and low flow regime by varying patterns of  $K_r$  heterogeneity throughout the simulation. The impacts of the pattern of  $K_r$  heterogeneity for the low flow regime are slightly expressed in stream depletion estimation results when the pattern of  $K_r$  heterogeneity for the high flow regime is assumed to occur on a quarter-year basis. Assuming half-year variations between the patterns of  $K_r$  heterogeneity for the high and low flow regime further reduce the impact of the individual flow regimes on stream depletion estimations.

## 4.4 Future Work

In this work we demonstrate how model input parameters determine the range of  $K_r$  to which numerical stream depletion estimations are sensitive. We also show how modeling  $K_r$  heterogeneity along the stream channel can potentially impact the feasibility of new pumping well locations. Our work offers an approach for modeling the streambed in numerical stream depletion estimations that is more complex than the standard method. However, the use of more sophisticated computer programs, such as HydroGeoSphere (HGS), may be necessary to overcome the limitations discussed in Section 4.2.

It would be valuable to further our understanding of the impacts of  $K_r$  heterogeneity on stream depletion estimations using HGS. Brunner (2010) demonstrates that HGS is capable of accounting for flow in the unsaturated zone, complex streambed heterogeneity, and vertical variations in hydraulic head. HGS could be used to develop a more complex and comprehensive model that accounts for  $K_r$  heterogeneity across the width and length of the streambed. This would allow for the input of  $K_r$  field measurements into a numerical stream depletion simulation. The resulting model would be able to more accurately depict the degree of stream depletion caused by pumping at various well locations in the model domain.

Additional future work could be done to compare the HGS and MODFLOW-2000 stream depletion simulation results. Considering the widespread use of MODFLOW-2000 for estimating stream depletion, it would be useful to understand how significant the differences are between the results of the two programs. The HGS results could be used to prove or disprove the validity of the simplifying assumptions made by MODFLOW-2000 for estimating stream depletion. The development of methods that simplify streambed heterogeneity in MODFLOW-2000, similar to the ones described in this work, could also be directed using simulation results from HGS.



## Bibliography

- [1] Andrews, E.D. (1979). Scour and Fill in a Stream Channel, East Fork River, Western Wyoming. U.S. Geological Survey, Geological Survey Professional Paper 1117, Reston, Virginia.
- [2] Barlow, P.M. and S.A. Leake (2012). Streamflow Depletion by Wells - Understanding and Managing the Effects of Groundwater Pumping on Streamflow. U.S. Geological Survey, Circular 1376, Reston, Virginia.
- [3] Brookshire, D.S, H. S. Burness, J.M. Chermak and K. Krause (2002). Western urban water demand. Natural Resources Journal, 42, 873-898.
- [4] Brunner, P., C.T. Simmons, P.G. Cook, and R. Therrien (2010). Modeling surface water-groundwater interaction with MODFLOW: some considerations. Ground Water, 48(2), 174-180.
- [5] Butler, J.J., V.A. Zlotnik, and M.S. Tsou (2001). Drawdown and stream depletion produced by pumping in the vicinity of a partially penetrating stream. Ground Water, 39(5), 651-659.
- [6] Butler, J.J., X. Zhan, and V.A. Zlotnik (2007). Pumping-induced drawdown and stream depletion in a leaky aquifer system. Ground Water, 45(2), 178-186.
- [7] Calver, A., (2001). Riverbed permeabilities: information from pooled data. Ground Water, 39(4), 546-553.
- [8] Cardenas, B.M., and V.A. Zlotnik (2003). Three-dimensional model of modern channel bend deposits. Water Resources Research, 30(6), 1-7.
- [9] Cardenas, B.M., J.L. Wilson, and V.A. Zlotnik (2004). Impact of heterogeneity, bed forms, and stream curvature on subchannel hyporheic exchange. Water Resources Research, 40(W08307), 1-13.
- [10] Cardenas, B.M. (2009). Stream-aquifer interactions and hyporheic exchange in gaining and losing sinuous streams. Water Resources Research, 45 (W06429), 1-13.
- [11] Cheng, C., J.S. Song, X. Chen, and D. Wang (2011). Statistical distribution of streambed vertical hydraulic conductivity along the Platte River, Nebraska. Water Resources Management, 25, 265-285.
- [12] Chen, X. and Y. Yin (1999). Evaluation of streamflow depletion for vertical anisotropic aquifers. Journal of Environmental Systems, 27(1), 55-60.

- [13] Chen, X. and Y. Yin (2001). Streamflow depletion: modeling of reduced baseflow and induced stream infiltration from seasonally pumped wells. Journal of the American Water Resources Association, 37(1), 185-195.
- [14] Chen, X. and L. Shu (2002). Stream-aquifer interactions: evaluations of depletion volume and residual effects from groundwater pumping. Ground Water, 40(3), 284-290.
- [15] Chen, X. (2004). Streambed hydraulic conductivity for rivers in south-central Nebraska. Journal of the American Water Resources Association, 561-573.
- [16] Chen X., (2005). Statistical and geostatistical features of streambed hydraulic conductivities in the Platte River, Nebraska. Environmental Geology, 48, 693-701.
- [17] Chen, X., M. Burbach, C. Cheng (2008). Electrical and hydraulic vertical variability in channel sediments and its effects on streamflow depletion due to groundwater extraction. Journal of Hydrology, 352, 250-266.
- [18] Chenpeng, L., X. Chen, G. Ou, C. Cheng, L. Shu, D. Cheng, and E.K. Appiah-Adjei (2011). Determination of the anisotropy of an upper streambed layer in east-central Nebraska, USA. Hydrogeology Journal, 20, 93-101.
- [19] Christensen, S. (2000). On the estimation of stream flow depletion parameters by drawdown analysis. Ground Water, 28(5), 726-734.
- [20] Clayton, J.A., and J. Pitlick (2007). Spatial and temporal variations in bed load transport intensity in a gravel river bend. Water Resources Research, 43(W02426), 1-13.
- [21] Conrad, L.P. and M.S. Beljin (1996). Evaluation of an induced infiltration model as applied to glacial aquifer systems. Water Resources Bulletin, 32(6), 1209-1220.
- [22] Doppler, T., H.H. Franssen, H.P. Kaiser, U. Kuhlman, and F. Stauffer (2007). Field evidence of a dynamic leakage coefficient of modelling river-aquifer interactions. Journal of Hydrology, 347, 177-187.
- [23] Fleckenstein, J.H., R.G. Niswonger, and G.E. Fogg (2006). River-aquifer interactions, geologic heterogeneity and low-flow management. Ground Water, 44(6), 837-852.
- [24] Genereux, D.P., S. Leahy, H. Mitasova, C.D. Kennedy and D.R. Corbett (2008). Spatial and temporal variability of streambed hydraulic conductivity in West Bear Creek, North Carolina, USA. Journal of Hydrology, 358, 332-353.
- [25] Glover, R.E. and G.G. Balmer (1954). River depletion resulting from pumping a well near a river. Transactions, American Geophysical Union, 35(3), 468-470.
- [26] Griebing, S.A. (2012). Quantification of stream depletion due to aquifer pumping using adjoint methodology (Masters Thesis). University of Colorado, Boulder, CO.
- [27] Griebing, S.A. and R.M. Neupauer (2013). Adjoint modeling of stream depletion in groundwater-surface water systems, Water Resources Research, in press.
- [28] Hansen, J.K. (2012). The economics of optimal urban groundwater management in the southwestern USA. Hydrogeology Journal, 20, 865-877.

- [29] Hantush, M.S. (1965). Wells near streams with semipervious beds. Journal of Geophysical Research, 70(12), 2829-2838.
- [30] Harbaugh, A.W., E.R. Banta, M.C. Hill, and M.G. McDonald (2000). MODFLOW-2000, The U.S. Geological Survey Modular Ground-Water Model, User Guide to Modularization Concepts and the Ground-Water Flow Process, U.S. Geological Survey, Open-File Report 00-92, Reston, Virginia.
- [31] Harvey, J.W. and K.E. Bencala (1993). The effect of streambed topography on surface-subsurface water exchange in mountain catchments. Water Resources Research, 29(1), 89-98.
- [32] Hunt, B. (1999). Unsteady stream depletion from ground water pumping. Ground Water, 37(1), 98-102.
- [33] Hunt, B. (2003). Unsteady stream depletion when pumping from semiconfined aquifer. Journal of Hydrologic Engineering, 12-19.
- [34] Hunt, B. (2009). Stream depletion in a two-layer leaky aquifer system. Journal of Hydrologic Engineering, 895-903.
- [35] Irvine, D.J., P. Brunner, H.H. Franssen, and C.T. Simmons (2012). Heterogeneous or homogeneous? Implications of simplifying heterogeneous streambeds in models of losing streams. Journal of Hydrology, 424-425, 16-23.
- [36] Kenny, J.F., N.L. Barber, S.S. Hutson, K.S. Linsey, J.K. Lovelace and M.A. Maupin (2009). Estimated Use of Water in the United States in 2005. U.S. Geological Survey, Circular 1344, Reston, Virginia.
- [37] Lambert, P.M., T. Marston, B.A. Kimball, and B.J. Stolp (2011). Assessment of Groundwater/Surface Water Interaction and Simulation of Potential Streamflow Depletion Induced by Groundwater Withdrawal, Uinta River near Roosevelt, Utah, U.S. Geological Survey, Scientific Investigations Report 2011-5044, Reston, Virginia.
- [38] Leake, S.A., D.R. Pool and J.M. Leenhouts (2008). Simulated Effects of Ground-Water Withdrawals and Artificial Recharge on Discharge to Streams, Springs, and Riparian Vegetation in the Sierra Vista Subwaterhead of the Upper San Pedro Basin, Southeastern Arizona, U.S. Geological Survey, Scientific Investigations Report 2008-5207, Reston, Virginia.
- [39] Levy, J., M.D. Birck, S. Mutiti, K.C. Kilroy, B. Windeler, O. Idris, and L.N. Allen (2011). The impact of storm events on a riverbed system and its hydraulic conductivity at a site of induced infiltration. Journal of Environmental Management, 92, 1960-1971.
- [40] MacDonald, G.M. (2010). Water, climate change, and sustainability in the southwest. Proceedings of the National Academy of Sciences, 107(50), 21256-21262.
- [41] Moore, J.E. and C.T. Jenkins (1966). An evaluation of the effect of groundwater pumpage on the infiltration rate of a semipervious streambed. Water Resources Research, 2(4), 691-696.
- [42] Mutiti, S. and J. Levy (2010). Using temperature modeling to investigate the temporal variability of riverbed hydraulic conductivity during storm events. Journal of Hydrology, 388, 321-334.

- [43] National Groundwater Association (2010). Groundwater Facts, <http://www.ngwa.org/fundamentals/use/pages/groundwater-facts.aspx>.
- [44] Neilson, M.G. and D.B. Locke (2012). Simulation of Groundwater Conditions and Streamflow Depletion to Evaluate Water Availability in a Freeport, Maine, Watershed, U.S. Geological Survey, Scientific Investigations Report 2011-5227, Reston, Virginia.
- [45] Neupauer, R. M. and S.A. Griebing (2012). Adjoint simulation of stream depletion due to aquifer pumping. Ground Water, 50(5), 746-753.
- [46] Palmer, M.A. (1993). Experimentation in the hyporheic zone: challenges and prospectus. Journal of the North American Benthological Society, 12(1), 84-93.
- [47] Ryan, R.J. and M.C. Boufadel (2006). Evaluation of streambed hydraulic conductivity heterogeneity in an urban watershed. Stochastic Environmental Research and Risk Assessment, 21, 309-316.
- [48] Scanlon B.R., C.C. Faunt, L. Longuevergne, R.C. Reedy, W.M. Alley, V.L. McGuire, and P.B. McMahon (2012). Groundwater depletion and sustainability of irrigation in the US High Plains and Central Valley. Proceedings of the National Academy of Sciences, 109(24), 9320-9325.
- [49] Sear, D.A. (1996). Sediment transport processes in pool-riffle sequences. Earth Surface Processes and Landforms, 21, 241-262.
- [50] Simpson, S.C. and T. Meixner (2012). Modeling effects of floods on streambed hydraulic conductivity and groundwater-surface water interactions. Water Resources Research, 48(W02515), 1-13.
- [51] Sophocleous, M., M.A. Townsend, L.D. Vogler, T.J. McClain, E.T. Marks and G.R. Coble (1988). Experimental studies in stream-aquifer interaction along the Arkansas River in central Kansas - field testing and analysis. Journal of Hydrology, 98, 249-273.
- [52] Sophocleous, M., A. Koussis, J.L. Martin, S.P. Perkins (1995). Evaluation of simplified stream-aquifer depletion models for water rights administration. Ground Water, 33(4), 579-588.
- [53] Sophocleous, M. (2002). Interactions between groundwater and surface water: the state of the science. Hydrogeology Journal, 10, 52-67.
- [54] Spalding, C.P. and R. Khaleel (1991). An evaluation of analytical solutions to estimate drawdowns and stream depletion by wells. Water Resources Research, 27(4), 597-609.
- [55] Springer, A.E., W.D. Petroustson, and B.A. Semmens (1999). Spatial and temporal variability of hydraulic conductivity in active reattachment bars of the Colorado River, Grand Canyon. Ground Water, 37(3), 338-344.
- [56] Sun, D. and H. Zhan (2007). Pumping induced depletion from two streams. Advances in Water Resources, 30, 1016-1026.
- [57] Taylor, R.G. (2012). Groundwater and climate change. Nature Climate Change, 1-8.

- [58] Theis, C.V. (1941). The effect of a well on the flow of a nearby stream. Transactions, American Geophysical Union, 22, 734-738.
- [59] Treese, S., T. Meixner, and J.F. Hogan (2009). Clogging of an effluent dominated semiarid river: a conceptual model of stream-aquifer interactions. Journal of the American Water Resources Association, 45(4), 1047-1062.
- [60] Ward, N.D. and H. Lough (2011). Stream depletion from pumping a semiconfined aquifer in a two-layer leaky aquifer system. Journal of Hydrologic Engineering, 16, 955-959.
- [61] Yeh, H.D., Y.C. Chang, and V. A. Zlotnik (2008). Stream depletion rate and volume from groundwater pumping in wedge-shape aquifers. Journal of Hydrology, 349, 501-511.
- [62] Zlotnik V.A., H. Huang (1999). Effect of shallow penetration and streambed sediments on aquifer response to stream stage fluctuations (analytical model). Ground Water, 37(4), 599-605.
- [63] Zlotnik, V.A. (2004). A concept of maximum stream depletion rate for leaky aquifers in alluvial valleys. Water Resources Research, 40 (W06507), 1-9.
- [64] Zlotnik, V.A. and D.M. Tartakovsky (2008). Stream depletion by groundwater pumping in leaky aquifers. Journal of Hydrologic Engineering, 13(2), 43-50.